Deliverable 4.10.5.3 Reflective Cracking Phase III Comprehensive Report

Delivery Order 015: Reflective Cracking Support

www.its.dot.gov/index.htm
Final Report — February 2017
######

U.S. Department of Transportation

Produced by (DTFACT-15-D-00007)
U.S. Department of Transportation
Office of the Assistant Secretary for Research and Technology
(List all USDOT agencies sponsoring this report; only list one agency on the report cover)

Notice

This document is disseminated under the sponsorship of the Department of Transportation in the interest of information exchange. The United States Government assumes no liability for its contents or use thereof.
The U.S. Government is not endorsing any manufacturers, products, or services cited herein and any trade name that may appear in the work has been included only because it is essential to the contents of the work.

Technical Report Documentation Page

1. Report No. **FHWA-JPO-XXXX**	**2. Government Accession No.** (Remove; Insert Information Here or leave blank)	**3. Recipient's Catalog No.** (Remove; Insert Information Here or leave blank)
4. Title and Subtitle **Deliverable 4.9.1 Standard Analysis/Report Template**		**5. Report Date** April 2016 **6. Performing Organization Code** (Remove; Insert Information Here or leave blank)
7. Author(s) **Hao Yin, Ph. D., P.E.** **Renaldo Aponte-CSRA** **Ryan Rutter-FAA** **Richard JI-FAA**		**8. Performing Organization Report No.** (Remove; Insert Information Here or leave blank)
9. Performing Organization Name And Address SRA International, Inc, A CSRA Company 1201 New Road Ste 242 Linwood, NJ 08221		**10. Work Unit No. (TRAIS)** (Remove; Insert Information Here or leave blank) **11. Contract or Grant No.** DTFACT-15-D-00007
12. Sponsoring Agency Name and Address (Remove; Insert Information Here or leave blank)		**13. Type of Report and Period Covered** (Remove; Insert Information Here or leave blank) **14. Sponsoring Agency Code** (Remove; Insert Information Here or leave blank)

15. Supplementary Notes

David Traverzo, Instrumentation Engineer from CSRA, was responsible for installing and maintaining all instrumentation used in this Test Phase of the Reflective Cracking Project.

Henry Fermin, Instrumentation Technician from CSRA, assisted with the installation of the Reflective Cracking Instrumentation.

16. Abstract

17. Key Words (Remove; Insert Information Here or leave blank)	**18. Distribution Statement** (Remove; Insert Information Here or leave blank)

19. Security Classif. (of this report) (Remove; Insert Information Here or leave blank)	**20. Security Classif. (of this page)** (Remove; Insert Information Here or leave blank)	**21. No. of Pages** (Remove; Insert Information Here or leave blank)	**22. Price** (Remove; Insert Information Here or leave blank)

Form DOT F 1700.7 (8-72) **Reproduction of completed page authorized**

Acknowledgements

Table of Contents

NOTICE I
Acknowledgements iii
Table of Contents iv
Executive Summary 1
INTRODUCTION 1
OBJECTIVE 2
REFLECTIVE CRACKING MITIGATION 2
Break/Crack and Seat, and Rubblization 2
Saw and Seal 3
Thick HMA Overlay 3
Mixture Modification 3
Reinforcement of HMA Overlay 4
Interlayer System 5
Stiff (Reinforcing) Interlayer 5
Soft (Strain Relieving) Interlayer 6
SELECTION OF MITIGATION TECHNIQUE 8
STRAIN RELIEVING INTERLAYER 9
Parametric Analysis Using Finite Element Analysis 9
HMA Mix Design 14
EVALUATION OF INTERLAYER MIX 15
Texas Overlay Tester 15
Complex Modulus 15
Disk-Shaped Compact Tension 19
OVERLAY STRUCTURE, CONSTRUCTION, AND INSTRUMENTATION 19
FULL-SCALE TEST 22
Performance of Fiber Optic Strain Sensor 22
Comparison of FEA and Field Responses 22
Crack Initiation 24
Crack Propagation 27
CONCLUSIONS 29
DATA STORAGE AND ORGANIZATION 30
REFERENCES 31

List of Tables

Table 1. Aggregate Properties. 14
Table 2. Aggregate Gradation. 14
Table 3. Volumetrics of Interlayer Mixes. 15
Table 4. Overlay Test Results. 16
Table 5. Dynamic Modulus Data. 16
Table 6. Summary of Sensor Location and Cycle to Failure. 21

List of Figures

Figure 1. Summary of FE Simulations. 12
Figure 2. FEA Results. 13
Figure 3. Master Curve for Mix A. 17
Figure 4. Master Curve for Mix B. 18
Figure 5. Dynamic Modulus Master Curves at a Reference Temperature of 77°F. 19
Figure 6. Fracture Test Results. 20
Figure 7. Strain Sensor Layout. 22
Figure 8. Fiber Optic Strain Sensor. 23
Figure 9. Comparison of FEA and Field Responses. 24
Figure 10. Strain Response History Plot. 25
Figure 11. Crack Initiation. 26
Figure 12. Crack Propagation. 27
Figure 13. Failure Observation. 29

Executive Summary

To protect the structure, extend service life, and restore a smooth riding surface, many airports repair deteriorating concrete pavements with an overlay of hot mix asphalt (HMA). Reflective cracking is a serious concern associated with the use of thin overlays but is not addressed in the current Federal Aviation Administration (FAA) Advisory Circular for asphalt concrete (AC) overlaid rigid pavements. This report presents a comprehensive study to quantify the crack initiation and propagation of a test HMA overlay with and without a strain relieving interlayer, and to evaluate the interlayer performance to retard thermally-induced reflection cracks. To achieve these objectives, three-dimensional finite element analyses (FEA) were first conducted to assess key structural parameters controlling the tension stresses at the overlay bottom. Next, laboratory tests were performed to certify fatigue, fracture, and viscoelastic performance of the interlayer mixture. Finally, a test pavement was built, instrumented, and tested at the FAA National Airport Pavement Test Facility (NAPTF). Full-scale test data suggested that the strain relieving interlayer considerably improved the reflective cracking resistance of the HMA overlay. Inclusion of a 1-in.-thick interlayer between existing concrete slabs and the overlay extended overlay service life regarding reflective cracking up to 15%. The intact interlayer had prevented spalling and moisture infiltration at the joint and therefore prolonged the structural integrity of the pavement. In addition, mixed-mode fracture and channeling were observed in the crack propagation.

INTRODUCTION

One of the maintenance challenges that airports face is overlaying existing airport pavements. For a moderately deteriorated portland cement concrete (PCC) pavement where jet blast and fuel spillage are not a major concern, resurfacing the existing pavement with a relatively thin hot mix asphalt (HMA) layer provides an economic means of restoring or improving pavement life. However, the new asphalt concrete (AC) overlay often fails before reaching its full design life due to the occurrence of reflective cracking. Nunn [1] pointed out the three mechanisms that start this reflection: fatigue due to thermal action (which produces expansion and contraction movements in the old layer), fatigue due to thermal shrinkage (because of the thermal gradient variations throughout the pavement) and fatigue caused by the action of traffic. Some researchers consider that the most important effect is achieved by the opening of the cracks, Mode I, while other consider that in Mode II, shear stresses due to load transfer between edges are more damaging. In the early stages of development, reflection cracks may barely be visible and are not considered to be a structural problem. However, when they propagate through the pavement, infiltration of water can weaken the foundation and fine material may be pumped to the surface, resulting in the creation of voids beneath the concrete. Traffic loading exacerbates the situation but of greater concern on airfields is the likelihood of spalling at the cracks and the potential for FOD (foreign object debris) damage to aircraft. Field experiences indicate that reflective cracks usually propagate to the pavement surface at a rate of approximately 1 inch per year and appear at the surface, in most cases, within three years or less (2). Unfortunately, the current Federal Aviation Administration (FAA) Advisory Circular for AC overlaid rigid pavements does not address reflective cracking (3).

The paving industry has seen dramatic increases in materials costs in the past 15 years. The U.S. Department of Energy (4) was projecting a 60 percent increase in world oil consumption from 1997 to 2020. Correspondingly, costs associated with constructing and maintaining pavements, and reducing the risk of FOD will undoubtedly continue to increase. Therefore, methods to extend pavement service life are becoming increasingly important. The economic benefits of reducing reflective cracking come from one or more of the following sources:

- increased life of the original pavement
- lower maintenance costs
- lower airport operation costs due to higher levels of serviceability
- lower traveler delay costs due to future preventive and rehabilitative maintenance interventions

According to Hughes and McGhee (5), the general belief among pavement engineers is that, even when a technique to delay reflective cracking is successful, the cost is equivalent to the cost of repairing the cracks. This opinion appears misleading if the appearance of the reflection cracking a few months after application of the overlay is considered. In addition, there is an inherent benefit associated with the measurement and treatment of cracking, since the cost of measurement of existing cracks and treatment will also have to be considered. For instance, Shalaby and Fréchette showed that an increase in crack spacing from 16.5 feet, occurring at the normal design life of 15 years, to 65.8 feet would extend the life to 20 years (6). With a reduction of crack spacing from 16.5 feet to 65.8 feet, Wei and Tighe (7) estimated a cost savings of $25,000 per two-lane kilometer.

An ongoing project sponsored by the FAA led to the development of the Temperature Effect Simulation System (TESS). The latest TESS upgrade was the installation of load cells that can measure actual forces being applied to a test HMA overlay. This report describes the finite element analyses, laboratory characterization, and full-scale tests involved in Phase III Test.

OBJECTIVE

One interesting observation from the Phase II Test was that the crack length progressed aggressively once the crack reached the middle of the overlay. This observation implies that, given a specific pavement structure and materials, the critical zone to retard bottom-up cracks is the lower portion of the overlay. The objective of the Phase III Test was to identify an appropriate mitigation technique to retard thermally-induced reflective cracking and to evaluate its effectiveness under full-scale test conditions.

REFLECTIVE CRACKING MITIGATION

Since the early 1930s, considerable resources and efforts have been spent to find new and relatively inexpensive techniques to delay reflective cracking (8). These techniques vary from simply increasing the AC overlay thickness to crack arresting interlayer to a three-ply composite that is placed only over the joint/crack area. Although some of these techniques have been successful for mitigating reflection cracks in certain applications, many have performed poorly, particularly in colder climates (9-10). This section summarizes a thorough literature review of commonly used mitigation techniques for reflective cracking for both highway and airport pavements:

- break/crack and seat, and rubblization
- saw and seal
- thick HMA overlay
- mixture modification
- reinforcement of HMA overlay
- interlayer system

Of all of the above techniques, rubblization, when done correctly, is the only direct method for the complete elimination of reflective cracking potential. On the other hand, rubblization is also the method which most closely resembles reconstruction, since a relatively thick overlay is required to compensate for the reduction in structural support resulting from the elimination of PCC slabs. A thick HMA overlay is well accepted as the least cost effective alternative.

Break/Crack and Seat, and Rubblization

The Department of the Air Force (11) recommends three procedures to retard reflective cracking. The crack or break and seat technique produces shorter slabs (2-6 feet), while retaining structural integrity by inducing fine, vertical, transverse cracks in the jointed concrete pavement. As the size of the slabs is effectively reduced, the horizontal strains resulting from thermal movements are distributed more evenly over the pavement and are therefore less likely to cause reflection cracks in the asphalt overlay. In a recent study (12), Ellis et al. reported the crack and seat with smaller bay sizes (1x1 foot) give a significantly lower risk of reflection cracking when overlaid.

Rubblization breaks or pulverizes the existing PCC pavement into small, interconnected pieces (having a nominal maximum size between 3 and 8 inches) that serve as a base course for the HMA overlay. In the past 7 years, more than one-half million square meters of airport PCC pavement has been rubblized, and overlaid with HMA (13). These projects range from heavy load military airfields to local general aviation (GA) airfields that handle small aircraft.

Because there are no hauling or disposal costs and none of the existing pavement system is discarded, these techniques and rubblization save natural resources, save landfill space, expedite construction, and are environmentally-friendly and cost-effective as a rehabilitation course of action. The existing PCC pavement stays in place and becomes the base for the new HMA pavement, thereby reducing or eliminating the need for new virgin aggregates. Weather delays are minimized since the subgrade is never opened up and exposed to the elements.

Saw and Seal

A minimum 4-inch overlay is required for this three-step procedure. First, a straight clean joint is dry saw cut in the HMA overlay directly above the existing PCC joint. The cut is then cleaned with hot compressed air to get rid of all the dust particles, loose debris, and most importantly, moisture that clings to the walls of the groove. The final step is to seal the joints with a low-modulus rubberized sealant (14). Field experience suggested the saw cuts match the underlying joints within ± 1 in, otherwise one or two secondary cracks that are parallel to the sawed joint will form under repeated loadings (15). These secondary cracks can result in severe raveling and joint deterioration. Since water infiltration and the possible stripping of HMA accelerate pavement deterioration, sealing the overlay joints properly plays an instrumental role in extending pavement service life (15). An advantage of "saw and seal" is that the controlled saw cut is more effectively sealed than a self-propagating zigzag reflection crack.

Thick HMA Overlay

In order to reduce the stress and strain in the overlay to acceptable limits for delaying reflective cracks, a thick HMA overlay is often applied than that required for structural purposes alone. Although this option provides an added benefit of better thermal insulation to the concrete, which helps to reduce thermal movements, it is usually not cost effective. The field rule-of-thumb is that one added inch of HMA will at most delay reflection cracks by 2 years (16). On a negative note, increasing the surface elevation on airfields requires the other related features (such as lighting) to be also raised accordingly.

Mixture Modification

The crack resistance of HMA depends on the fracture properties. Improved fracture properties can be achieved by modifying the asphalt, using softer binder, and/or increasing the film thickness of asphalt. However, field experiences with such modifications have generally been unfavorable because the amount of strain that must be endured in localized areas (i.e., joints and cracks) is much greater than the tensile strain at failure for the softest asphalt. A number of studies showed that the use of stone matrix asphalt (SMA) and polymer modified asphalt (PMA) mixtures reduced surface distress (rutting, fatigue cracking, and thermal cracking) in comparison to dense-graded neat HMA mixtures. However, due to inadequate fracture resistance, SMA and PMA will reduce the severity of the reflective cracks, but not significantly delay those cracks from occurring. It should be pointed out that when these modified mixtures placed between the distressed pavement and the conventional HMA overlay, this interlayer absorbs a significant portion of the movement at the joints and, therefore, increases the pavement service life against reflective cracking (17). This observation could be attributed to the high asphalt content and admixtures, which allow the modified mixture to remain intact adjacent to the cracks.

Reinforcement of HMA Overlay

Two common types of reinforcement that have been used to mitigate reflection cracks are steel and geosynthetics. The idea is to increase the tensile strength of the overlay and to hold the cracks tightly together (relatively low severity) once they occur.

Steel reinforcement can be placed in narrow strips over the joints and cracks in the PCC pavement or continuously over the entire length of the project. Both welded wire fabric and expanded metal reinforcement has been used. In the U.S., the steel reinforcement netting interlayer system was first installed at the Virginia Smart Road in 1999 (18-19). Most studies have concluded that the use of steel reinforcement provided better performance than the control case. The primary disadvantage of steel reinforcement is that water within the HMA mixture causes the steel to corrode in as little as four years of service. Consequently, the reinforcement effectiveness might be reduced, as reported by Ellis et al. (12).

Geosynthetics is the collective term applied to sheets of synthetic polymer material incorporated in soils and pavements. Geosynthetics include fabrics, geotextiles, geogrids, and composites. Fabrics or geotextiles may be woven or nonwoven and are typically composed of thermoplastics such as polypropylene or polyester but can also contain nylon, other polymers, natural organic materials, or fiberglass (20). These materials are hypothesized to improve HMA overlay performance through the following mechanisms: reinforcing the overlay, relieving the stress/strain concentrations at joints and cracks, and reducing surface water infiltration to the lower layers. The performance of geosynthetics in mitigating reflection cracks in HMA overlays has ranged from successes to failure. As reported in AAPTP 05-04 (13), most studies have concluded that the cost effectiveness of geosynthetics in mitigating reflective cracks is marginal at best. However, these materials do keep the widths of the reflective cracks narrower during the winter months when used as a reinforcing material.

Ahlrich (21) developed a map with climatic zones as a guide to paving fabric performance and did not recommend paving fabrics for northern states. Similarly, Buttlar et al. (22) showed that geotextiles can delay reflective cracking for a few years at airports in warmer climates; however, the same geotextiles cannot delay reflective cracking to the same degree at locations with colder climates. This may be explained by the fact that much of the cold-weather contraction and cracking occurred within the overlay, over the paving fabric, and was not reflected from lower layers. It should, however, be noted that the waterproofing effects can still provide long-term benefit by controlling the moisture content in the lower layer. Maurer and Malashekie (23) conducted a 10-year life-cycle analysis in Pennsylvania in which six treated test sections (with paving fabrics) were compared with control sections. Four different paving fabrics, as well as two polymer-modified AC mixtures, were used. The selected fabrics were non-woven, needle-punched, spunbonded polyester and polypropylene. This 44-month monitoring project showed that the use of fabrics did not reduce life cycle costs when overlaying PCC with asphalt. Based on a study on the effectiveness of paving fabrics to reduce reflective cracks in the U.S. and foreign countries, Amini (24) concluded that paving fabrics offer little benefit for thin overlays (less than 2 in), but for thicker overlays their performance has been successful for the most part. In general, paving fabrics have performed considerably better in warm and mild climates than in cold ones (25).

Button (26) concluded that the use of geotextiles on Texas PCC (continuously reinforced) pavements did not provide any additional benefit in minimizing reflective cracking caused by thermal gradients (horizontal expansion and contraction of PCC slab). Bozkurt et al. (27) found that the use of geotextiles in Illinois only slightly retarded the reflective cracking on the longitudinal joints and were ineffective at retarding the reflective

cracking on the transverse joint. Shuler and Harmelink (28) compared two different Petromats, a geotextile, a reinforced fabric, and a fiberglass tape to two control sections in Colorado. The sections were monitored for 5 years and concluded that the control sections (4 and 5.5 in thick HMA overlay, respectively) provided the most cost effective method.

In 2000, the Maine DOT experimented with a GlasGrid 8502 on runway 17-35 of the Auburn-Lewiston Municipal Airport to determine its effectiveness in reducing reflective cracking of the subsequent HMA overlay (29). After 4.6 years, Maine DOT observed significant cracking in both the test and control sections and determined that most of it was reflective cracking. They found that the geosynthetic did not significantly reduce reflective cracking in this case. However, they pointed out that there were serious installation concerns due to inadequate adhesion of the GlasGrid to the runway, overbanding of crack sealant, and subsequent paving difficulties caused by the overbanding. These concerns prevented meaningful conclusions on the effectiveness of the product.

Composites consist of fabric laminated onto a grid. The fabric permits adhesion of the composite onto a pavement surface, and the grid provides strength and stiffness. Ramsamooj and Gabriel (30) compared fiberglass composite overlays to standard FAA specification for rehabilitation of an airport runway using a 12 in overlay. The aircraft used in the study was a Boeing 777 with a 6-wheel gear load, each wheel weighing 64 kips with a tire pressure of 200 psi. Both aircraft loading and thermal stresses were considered in the theoretical comparison. Wire mesh reinforcement at the mid depth of the HMA was used above the cracks and joints to enhance the shear strength of the overlay. The results showed that the standard overlay would develop reflective cracking after 6.5 years, and complete failure of the subgrade under the joints and cracks was expected after 10.5 years. The new fiberglass composite overlay appeared capable to sustain aircraft loadings throughout the entire design life of the PCC runway.

Interlayer System

Starting from the early 1960s, extensive research studies have reported on the effectiveness of interlayer systems to reduce the occurrence of reflective cracking and have explored their cost effectiveness. Depending on its intended function, the interlayer system can vary. According to Button and Lytton (31), reinforcement of HMA with a stiff interlayer provides a better distribution of the applied load over a larger area and compensates for the lack of tensile strength of the HMA. Geogrid, made from high-density polypropylene or polyethylene with an open mesh structure, fiberglass grids, and metallic grids are examples of reinforcing layers that are sometimes used in HMA overlay systems. On the other hand, strain relieving interlayers, dissipates strain energy in the vicinity of the crack through the use of soft materials. Nonwoven geosynthetics, stress absorbing membrane interlayers (SAMIs), and proprietary composite material systems such as interlayer stress absorbing composite “ISAC”, are good examples of strain relieving interlayers. While the original SAMIs installed in the field were more akin to chip seals with a heavy tack coat application, more recently, thicker stress relief interlayer systems have gained popularity, which can be plant produced and constructed with standard HMA paving equipment (e.g. Sand Anti-Fracture (SAF) layer).

Stiff (Reinforcing) Interlayer

Based upon earlier work by Button, Lytton and Monismith (31-32), with a reinforcing interlayer, the reflection crack starts to propagate (due to thermal and traffic loading) from its original position upward until it reaches the interlayer. If the interlayer is stiff enough, the crack will turn laterally and moves along the interface until its

energy is exhausted. Lytton pointed out that the reinforcement failure would develop only after debonding has occurred between the lower layer and the interlayer. Note that reinforcement can only occur if the interlayer is sufficiently thick and is stiffer than the surrounding materials. Given a reinforcing interface may contribute to the structural capacity of the pavement; it is realistic to reduce the required thickness to reach the same level of performance.

Zhengpi and Dengliang evaluated the effectiveness of a reinforcing interlayer in preventing reflection cracking (33). In the test setup, two concrete slabs separated by a joint, were used to simulate thermal horizontal movement in rigid pavement. An HMA layer was then compacted on top of the concrete slabs to simulate an overlay. Reinforcement was placed between the two layers and testing was conducted at two temperatures: 14°F and room temperature. The overlay thickness was fixed at 2.75 in. The authors reported that reinforcement might improve the HMA resistance to reflective cracking by nearly tenfold. Moreover, monitoring of crack propagation during this test indicated that the reinforcement reduces stress concentration near the cracks, and therefore, retards reflection cracking.

Brown et al. (34) conducted various laboratory tests to identify the effectiveness of interlayer systems and develop a design procedure for reinforced flexible pavements. The authors found that all interlayers were effective in preventing reflective cracking due to the thermal movement of a concrete slab. Geogrid and glass fiber gave an improvement factor of up to eight.

Montestruque et al. evaluated the effectiveness of polyester geogrid in combating reflective cracking (35). Fatigue tests were conducted with and without reinforcement using HMA beams resting on an elastic rubber base support. The geogrid was placed right on top of a pre-crack. Failure was defined at the point in the test in which the crack appeared at the surface. Results of the experimental program showed that unreinforced beams failed quickly after the start of the test. The crack propagation process was vertical in both the bending and shearing modes. Reinforced beams only exhibited vertical growth up to 1.18 in.

Gallego and Prieto (36) developed a laboratory setup, the Wheel Reflective Cracking (WRC) device, to determine an overlay performance against reflective cracking with and without reinforcement. Of the two overlays without geosynthetics, the test results successfully predicted that the mix with polymer-modified binder would perform better than the mix with straight binder. The reinforced overlay performed better than the two unreinforced specimens did. The reinforced overlay had 1.5 times better strength than the polymer-modified overlay. At failure, the reinforced overlay exhibits failure over a large area while the unreinforced specimens exhibited one reflective crack at failure. This indicates that the presence of geosynthetics helps reduce the stress concentration near the crack and allows distributing the stresses over a wider area.

Soft (Strain Relieving) Interlayer

A strain relieving interlayer is a soft layer that is usually placed at the bottom of an HMA overlay to absorb a large portion of the energy, which would otherwise be part of the crack propagation process. Based upon earlier work by Button, Lytton and Monismith (31-32), with a strain relieving interlayer, the reflection crack starts to propagate (due to thermal and traffic loading) from its original position upward until it reaches the stress-relieving layer. Due to its low stiffness, the interlayer will exhibit large deformations, which will be accompanied with a dissipation of energy. The crack propagation will stop for a while due to the lack of energy, and then propagate from the top of the interlayer upward to the surface. Such “crack jumping” and “crack offsetting” mechanisms have been identified and observed in a number of studies (37-40). Monismith and Coetzee (32) associated the contribution of a strain relieving interlayer to the pavement system with what they called “a

crack arrest" phenomenon. Based on this mechanism, a soft interlayer is capable of redirecting the crack from its original direction to the horizontal plane. This phenomenon was also noticed by Majidzadeh when testing an HMA beam reinforced at mid depth using "Petromat" (41). Typical thickness of strain relieving interlay in airfields is either less than 2 in or greater than 3 in (13). The thin layers dissipate only the horizontal movements, while the thicker layers are hypothesized to dissipate both horizontal and differential vertical movements at joints and cracks. Two problems associated with thicker interlayers include: the total overlay thickness is generally much greater than for some of the other mitigation strategies, and if an open-graded HMA mixture is used, the interlayer can be a potential water conduit or reservoir between the overlay and existing pavement.

The use of a stain relieving interlayer has shown some promise in mitigating reflective cracking. In 1966, a crumb rubber HMA overlay at the Phoenix International Airport performed excellently (42). McLaughlin reported that the worst cases of reflective cracking were evident in airport pavements when a thin overlay (less than 2 in) was placed over a badly cracked HMA or PCC pavement. This investigation revealed that when a 4-inch overlay was feathered out to 2 in, reflective cracking appeared only in the areas of the thinner HMA.

In Arizona (43), a 200-300 penetration asphalt from the Los Angeles Basin (low temperature susceptibility) was used in a 1.26 in HMA overlay and then covered with an approximately 0.5 in HMA wearing surface. This structure-material combination was found to be one of the five most effective treatments to reduce reflection cracking.

The U.S. Army Corps of Engineers Waterways Experiment Station (44) evaluated an asphalt-rubber membrane and a non-woven fabric placed below a thin HMA overlay (2 in or less). Field tests of two asphalt-rubber membrane formulations and three nonwoven fabrics were placed on roads and airfield pavements at five Army installations in various areas of the United States. This system has been found to significantly delay reflective cracks from existing flexible pavements, but has been less effective when placed over existing JPCP or JRCP.

Sherman (45) reported on a project in Wyoming that included the use of a 2 in soft asphalt interlayer (viscosity grade, AC 2.5) and crack sealer. This system exhibited the least amount of cracking and was the most effective for reducing reflective cracking.

Patterson reported a study using a thin PMA included in a medium-thickness HMA overlay for the rehabilitation of cracked concrete pavements (46). This application has been also used below thin overlays with more severe surface conditions, such as joint movements of up to approximately 0.28 in under airport runway loadings. Results showed the crack resistance of the pavement structure was improved by increasing overlay thickness and stiffness and reducing the membrane stiffness. Theoretical analyses of this system indicated that a 3.15 in thick composite membrane-overlay system covered by an open-graded HMA overlay can satisfy the design requirements and is comparable to 9.4 in thick conventional overlay for control of crack reflection over a 15-year life. This type of interlayer was shown to be safe under all aircraft loading conditions, and has been successfully used.

New Mexico (47) studied the influence of variables such as rubber type, mixing temperature, batch repetition, and test temperature on cracking resistance. Four laboratory tests and a field trial were conducted. Results from a field experiment showed that the mixing time has a significant influence on cracking observed, while the rubber type showed no influence on cracking.

Barksdale (48) further indicated that, for pavements with light to moderate cracking, a crack filling program is likely more cost effective than other methods. He indicated that approaches such as full-width fabrics require

additional construction steps that, in turn, may reduce quality control and thus reduce overlay performance. Alternatives for reducing reflective cracking may include: softer asphalt and/or additives such as polymers, rubber, fibers, carbon black, or sulfur in the HMA overlay.

Dempsey presented the development and evaluation of the Interlayer Stress-Absorbing Composite (ISAC) system (49-51). ISAC is a three-ply composite interlayer usually placed as a 36 inch wide strip-type treatment over joints and cracks. The bottom non-woven geotextile layer is provided mainly for manufacturing purposes and to facilitate bonding between ISAC and the existing pavement. The viscoelastic membrane layer is designed to provide base isolation benefits due to its low modulus and high ductility even at very low pavement temperatures. This layer consists of a highly modified, elastomeric binder. Five ISAC test sections were placed between 1997 and 2000 (52). Some of these ISAC sections contain other reflective crack control methods, such as SAF layer and strip and area-wide reflective crack control fabric. For all five test sections, the formation of reflective cracks and the subsequent deterioration of these cracks were delayed at ISAC treated joints and cracks. This delay ranged from over one year to close to three years when compared to the untreated and other crack control methods. Recent studies by Al-Qadi et al. (53-54) showed clearly that ISAC can retard reflective cracking, but its cost effectiveness depends on the number of cracks or joints per lane length.

Extensive work by Blankenship (55) showed that as long as the interlayer mixture can obtain the required laboratory performance criteria, a 50% reduction in the average crack rate can be achieved. In fact, cores taken from a number of sites have shown that even when cracking occurred in the surface layer, the interlayer itself did not crack. The intact interlayer, compacted to low air void levels, further protects the pavement from moisture intrusion. A pilot study conducted in New Jersey in 1997 indicated that a 68% decrease in the average crack growth rate was achieved with the interlayer when compared to the control sections.

Elseifi and Al-Qadi (56) linked field observations and measurements to engineering theories to evaluate the effectiveness of a newly-developed geocomposite membrane, a PVC layer sandwiched between two layers of geotextile, as a strain energy absorber. The researchers concluded that when used in rehabilitated pavement, a low modulus interlayer is able to dissipate most of the available energy at the crack tip, therefore minimizing the potential of an existing crack reflecting into the overlay. A geocomposite membrane creates a protective shield around the crack tip, separating the criticality of the stress field in the cracked area from the bottom of the overlay. Moreover, a resultant compressive horizontal stress field helps close the crack rather than open it.

SELECTION OF MITIGATION TECHNIQUE

As mentioned previously, many mitigation techniques have been utilized to control reflective cracking in airport pavements. However, most of these techniques only briefly delay or limit the severity of the reflective cracks. Based on the literature review, some general observations and recommendations include:

- In general, break and seat has better results in JPCP than crack and seat for JRCP.
- Edge drains should be used in all rubblized projects to drain any saturated foundation layer.
- The “saw and seal” method is best suitable for JRCP with longer slab length with no mid slab cracking. Shorter slab length requires a large amount of sawing and sealing which may not be cost effective.
- Reinforced HMA overlay should not be laid atop JRCP and JPCP, especially when large differential vertical deflections and faulting occur at joints and cracks.
- Pneumatic rubber tired rollers should not be used in the primary or breakdown position when using some highly polymer modified mixtures, because the rubber tires pick up the material during the rolling process.

- When steel reinforcement is used for HMA overlays, any folds or wrinkles must be eliminated during placement.
- HMA overlays reinforced with steel cannot be milled.
- If softer asphalts are used as an interlayer, the HMA overlay must be thick and stiff enough to resist rutting and shoving under aircraft movements.
- Soft interlayer is not recommended to accommodate large differential vertical deflections across joints or cracks.

For Phase III Test, it was decided to evaluate the effectiveness of strain relieving interlayer to retard reflective cracking after the following factors were well-thought-out:

- Existing PCC pavement condition
  - No distresses (cracks and faulting)
  - Joint transfer, LTE > 0.85
  - No voids between the rigid bottom of TESS and the Teflon layer
- Research scope
  - TESS is designed to simulate temperature load only
  - Structural strengthening is not needed
  - Proprietary materials are not appropriate
- Construction constraint
  - Standard plant production and conventional paving operation are preferred
  - Break/Crack and Seat, and Rubblization are not applicable
  - Drainage are not applicable
  - Re-construction favors milling
- Field implementation
  - The overly should prevent rutting, slippage, shoving, and fatigue cracking
  - The elevation of the final pavement surface should be minimized
  - Additional drainage system should be avoided
  - The mitigation strategy should be cost-effective

STRAIN RELIEVING INTERLAYER

A strain relieving interlayer is usually positioned at the bottom of an HMA overlay to absorb a large portion of the energy, which would otherwise be part of the crack propagation process. The typical thickness of a strain relieving interlay in airfields is either less than 2 in. or greater than 3 in. (13). The thin layers dissipate only the horizontal movements, while the thicker layers are hypothesized to dissipate both horizontal and differential vertical movements at joints and cracks. Two problems associated with thicker interlayers include 1) the total overlay thickness is generally much greater than some of the other mitigation strategies employ, and 2) if an open-graded HMA mixture is used, the interlayer can be a potential water conduit or reservoir between the overlay and existing pavement.

Parametric Analysis Using Finite Element Analysis

Phase I test (57) revealed that the driving mode for bottom-up reflection cracks was fracture Mode I; therefore, the focus of finite element analysis (FEA) was placed on the horizontal tensile stresses at the overlay bottom. Yin (58) demonstrated a three-dimensional finite element (FE)-based pavement simulation model to analyze

thermally-induced reflective cracking. In the current study, a commercially available FE software package, ABAQUS, was used as the analysis engine. In the developed full-scale, three-dimensional (3-D) FE model, a generalized Maxwell model was used for the AC. The concrete layer and subgrade were modeled as linear elastic materials. This is a reasonable assumption because the stress state of granular layers typically involves low-magnitude triaxial compression under all applied field loads. The HMA overlay was fully bonded to the underlying slabs. No separation in normal direction was allowed once the two interfaces were contacted. The interface between concrete and subgrade was assumed to be frictionless. Yin (57, 60) reported that reflection cracks most likely initiated from the edge of pavement in full-scale tests. In order to generate maximum amount of information from one round of full-scale test, it was worth to evaluate another alternative, two-strip AC overlay. An illustration of this comprehensive model is given in figure 1a. A haversine function describing the relationship between the loading time and the joint opening was used to approximate the temperature variations. In this study, the same full-scale FE model was used to assess two key structural parameters of the interlayer: thickness and stiffness.

According to Von Quintus et al. (13), 4-in. dense-graded mixtures with adequate stability should be sufficient on GA facilities, while 6 in. should be sufficient for heavier aircraft at larger commercial aviation airports. For full-scale test purposes, the constructability and construction quality are critical. In addition, the overlay should not survive to a number of repetitions beyond the project time frame. Figure 1b shows three overlay thickness combinations proposed for the interlayer section. The control section contained 5-in.-thick standard FAA P-401 material. The main purpose of a strain relieving interlayer is to isolate relative displacements between the overlay and existing pavement, such that the longitudinal horizontal tensile stresses in the overlay caused by thermal cycling can be significantly reduced. To accomplish these characteristics at low temperatures (i.e., 32°F), the interlayer material must possess excellent strain relieving and have the ability to relax stresses rapidly. Two reduction levels were selected to represent the interlayer's softness, 75% and 50% of the overlay's relaxation modulus, *E(t)*. The relaxation modulus was obtained from the creep compliance test on standard FAA P-401 material. The relaxation modulus master curves at the reference temperature of 32°F are provided in figure 1c.

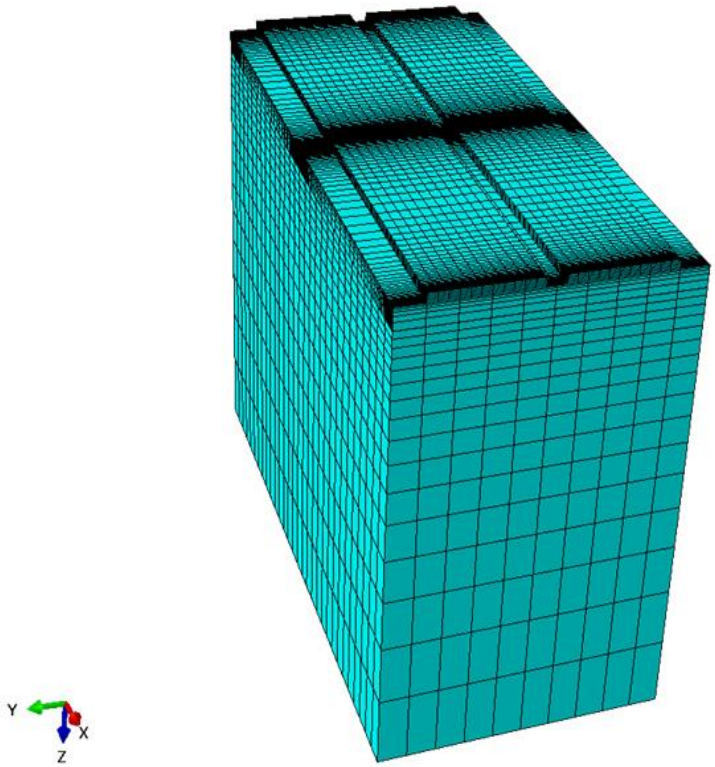

(a) Two-strip 3-D Finite element model

4.5” Overlay + 0.5” Interlayer

4.0” Overlay + 1.0” Interlayer

3.5” Overlay + 1.5” Interlayer

(b) Thickness combination

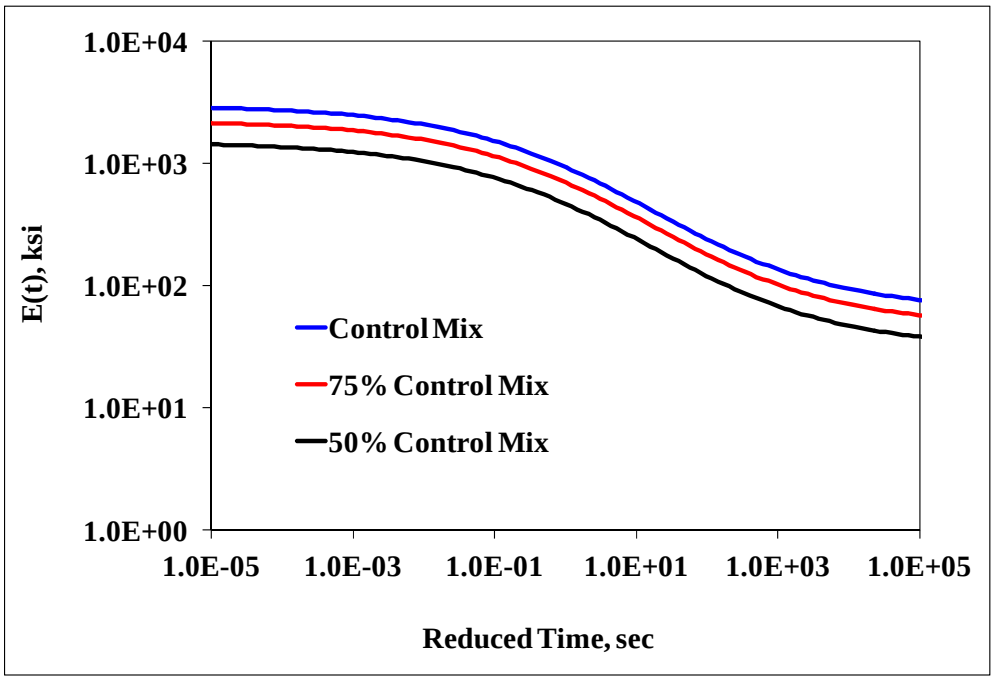

(c) Relaxation modulus master curves at a reference temperature of 32°F

Figure 1. Summary of FE Simulations.

Figure 2a shows the tensile stress distributions in the longitudinal direction. The tensile stress sharply declined from its peak value atop the joint toward the middle of the slab. For the control section, full (100%) HMA relaxation modulus resulted in the maximum tensile stress of 355 psi. With the inclusion of an interlayer, the stress magnitude was considerably reduced. At 75% of the HMA relaxation modulus, the maximum tensile stresses at the interlay bottom ranged from 277 to 300 psi. When the relaxation modulus was further reduced to 50%, the maximum tensile stress was only 40% of that in the control section, 150 psi. It is clear that, for the interlayer section, the interlayer stiffness had a much more pronounced influence on the tensile stresses compared to the thickness. The tensile stress distributions in the transverse direction are important for instrumentation (58). As shown in figure 2b, the tensile stresses reached peak values at 6 in. from the outer and inner edges for both the north and south strips. However, once the *E(t)* dropped to 50%, the tensile stresses at the interlayer bottom were nearly uniform. Like the longitudinal direction, the contribution to relieving tensile stress was predominantly from the reduction of HMA stiffness.

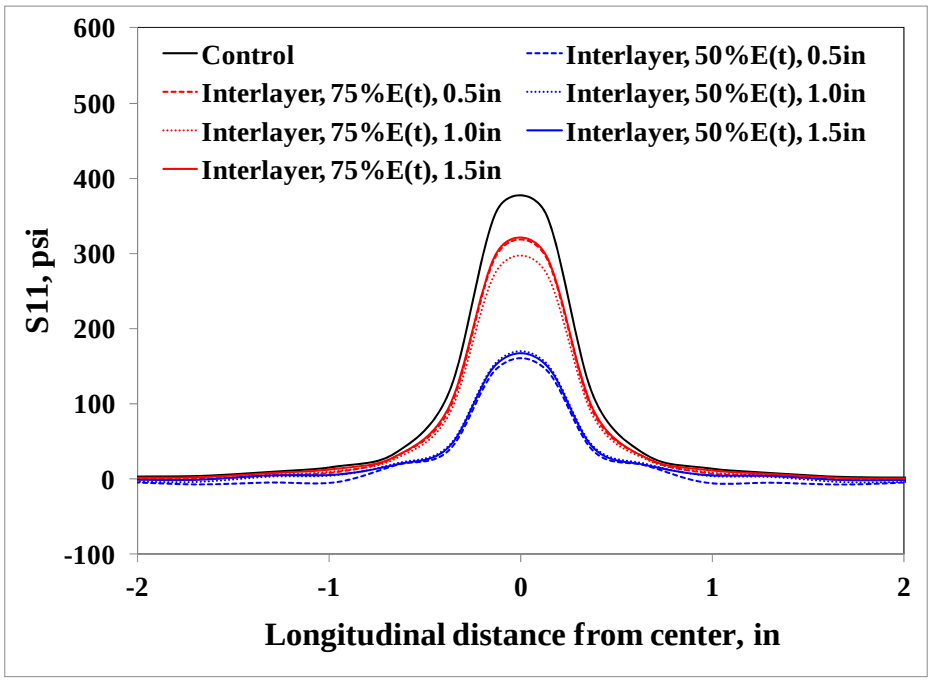

(a) Tensile Stress in Longitudinal Direction

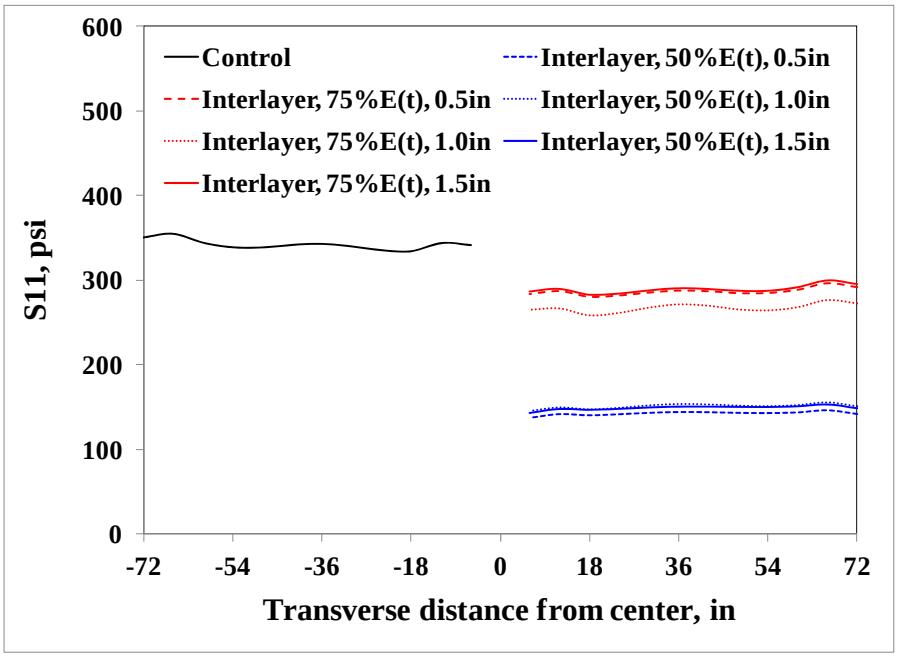

(b) Tensile Stress in Transverse Direction

Figure 2. FEA Results.

HMA Mix Design

The strain relieving interlayer is a fine graded, polymer modified asphalt (PMA), asphalt-rich mixture. The PMA is a cross-linked, elastomeric styrene-butadiene block copolymer system that is less susceptible to temperature and has a higher viscosity at ambient temperature compared to unmodified or neat asphalt mixtures. In addition, the PMA provides the elasticity to withstand and partially absorb the tension, shear, and bending exerted on the pavement. As FEA simulations demonstrated, a 1-in.-thick soft interlayer seemed promising to reduce the maximum tensile stress directly above the joint. Two interlayer mix designs were specifically developed using a PG 76-22 PMA following the Mix Specification (see Appendix A). Table 1 shows the source properties of the aggregates and table 2 shows the design gradation along with the specifications for blend A and blend B. The mixes were aged according to AASHTO R35, *Standard Practice for Superpave Volumetric Design for Hot Mix Asphalt* and compacted according to with AASHTO T-312, *Preparing and Determining the Density of Hot Mix Asphalt specimens by means of the Superpave Gyratory Compactor* at the design gyrations of 50. Table 3 shows the volumetrics for mix A and mix B. The PG grade of the binder utilized in this mix was PG 76-22. The mixing temperature was above 360°F and compaction temperature was above 275°F. All requirements were met except air voids for mix B. The initial design for mix B included a slightly higher binder content and met the air void requirement. However, the mix which was laid down as a test strip contained only 7.9% binder content.

Table 1. Aggregate Properties.

Rocktype / Material	carbonate	argillite
Size	#57	#57
%Abs	0.4	0.7
Bulk Sp. Gr.	2.829	2.694
SSD Sp. Gr.	2.84	2.711
App. Sp. Gr.	2.858	2.741
Unit Wt.	95	83
Voids	47	51
LA	32	14
ASR	0.02	0.03

Table 2. Aggregate Gradation.

Sieve Size	Aggregate Source			Cumulative Percent Passing	
	S-1	S-2	S-3		
	Dolomite	Dolomite	Argillite	Blend A	Blend B
	#9	#10	#10	(40% S-1 and 60% S-2)	(35% S-1, 20% S-2, and 45% S-3)
⅜ in. (9.5 mm)	100.0	100.0	100.0		
No. 4 (4.75 mm)	85.5	99.0	99.6	92.0	92.3
No. 8 (2.36 mm)	18.0	60.5	83.3	46.8	55.9
No. 16 (1.18 mm)	2.8	30.1	54.1	25.3	34.7

No. 30 (0.600 mm)	0.3	16.5	34.7	16.7	23.7
No. 50 (0.300 mm)	0.0	10.1	23.2	12.4	16.8
No. 100 (0.150 mm)	0.0	4.5	16.6	8.3	11.8
No. 200 (0.075 mm)	0.0	0.0	12.1	4.6	8.2
Pan	0.0	0.0	0.0	0.0	0.0

Table 3. Volumetrics of Interlayer Mixes.

Component	Mix B	Mix A
Binder (%)	7.9	8.2
Binder Requirement (%)	≥7	≥7
Maximum Specific Gravity	2.450	2.532
Bulk Specific Gravity	2.326	2.455
Air voids (%)	5.046	3.078
Air Void Requirement (%)	2.5-3.5	0.2-3.8
VMA (%)	20.48	16.36
VMA Requirement (%)	≥ 18	≥16

EVALUATION OF INTERLAYER MIX

To select an appropriate interlayer mix, laboratory tests were conducted to evaluate fatigue, fracture, and viscoelastic performance of HMA. These included Texas Overlay Tester, disk-shaped compact tension, and complex modulus tests. All test samples were 6-inches in diameter and laboratory prepared with target air voids of 7%.

Texas Overlay Tester

The test was performed at 77°F on laboratory prepared samples with 7% Air Voids using Tex-248-F *the Overlay Test* specification. Samples were cycled at 0.1 Hz in displacement control from 0 to 0.635mm. The average air voids percentages of the cut samples for mix A and mix B were 7.05% and 7.35% respectively. The test was set to terminate when either a 93% load reduction was reached or 1200 cycles completed. Five samples were tested from each mix design. Table 4 shows the overlay test results. All samples tested passed, reaching the 1200 cycle limit without experiencing a 93% reduction in load.

Complex Modulus

In addition to fatigue and fracture performance, it is also important to measure the bulk material viscoelastic properties, because the overall material response (stresses and strains) are governed by the bulk material characteristics. The dynamic complex modulus test is performed on laboratory compacted samples that have 7% air voids after being cored and cut to 150mm high and 100 mm diameter samples according to AASHTO T-342 Standard Method of Test for Determining Dynamic Modulus of Hot-Mix Asphalt Concrete Mixtures. Three samples were tested for each mix design. Four temperatures (10°, 40°, 70°, and 100°F) and three

loading frequencies (10, 1, and 0.1 Hz) were considered. Table 5 summarizes dynamic complex modulus test results for mix A and mix B. Figures 3 and 4 show phase angle and dynamic modulus master curve for mix A and mix B, respectively. Figure 5 shows the dynamic modulus (|E*|) master curves at a reference temperature of 70°F for all test samples. It appeared that the difference between mixes varied, but mix B was slightly stiffer than mix A at higher frequencies and much softer at lower frequencies. AC mixtures that exhibited lower stiffness properties at high frequencies (low temperatures) tended to be more crack resistant.

Table 4. Overlay Test Results.

Sample	Peak Load (kN)	Reduction in Load (%)	Pass (Y/N) (reduction in load <93% at 1200 cycles)
Mix B1	0.798	71.4	Y
Mix B2	0.885	72.5	Y
Mix B3	0.704	76.3	Y
Mix B4	0.697	79.2	Y
Mix B5	0.602	76	Y
Mix A1	0.486	73	Y
Mix A2	0.379	75.6	Y
Mix A3	0.589	72.0	Y
Mix A4	0.501	72.2	Y
Mix A5	0.409	73.3	Y

Table 5. Dynamic Modulus Data.

Conditions		A		B	
		Modulus	Phase Angle	Modulus	Phase Angle
Temperature	Frequency	Mean	Mean	Mean	Mean
°	Hz	Ksi	°	Ksi	°
-12.2	0.1	1723.33	12.87	1870.77	9.88
-12.2	1	2362.46	8.90	2410.33	7.10
-12.2	10	2834.36	6.56	2829.6	5.37
4	0.1	821.2	22.23	1005.7	17.13
4	1	1293	16.53	1448.13	13.01
4	10	1818.92	12.31	1916.53	10.07
20	0.1	158.62	35.01	259.47	29.99
20	1	368.00	31.73	507.03	25.49
20	10	733.79	25.70	873.47	20.24
40	0.01	10.55	22.22	22.03	25.92
40	0.1	20.13	28.35	41.57	30.52
40	1	49.12	35.14	91.6	33.60
40	10	135.59	39.02	212.6	33.82

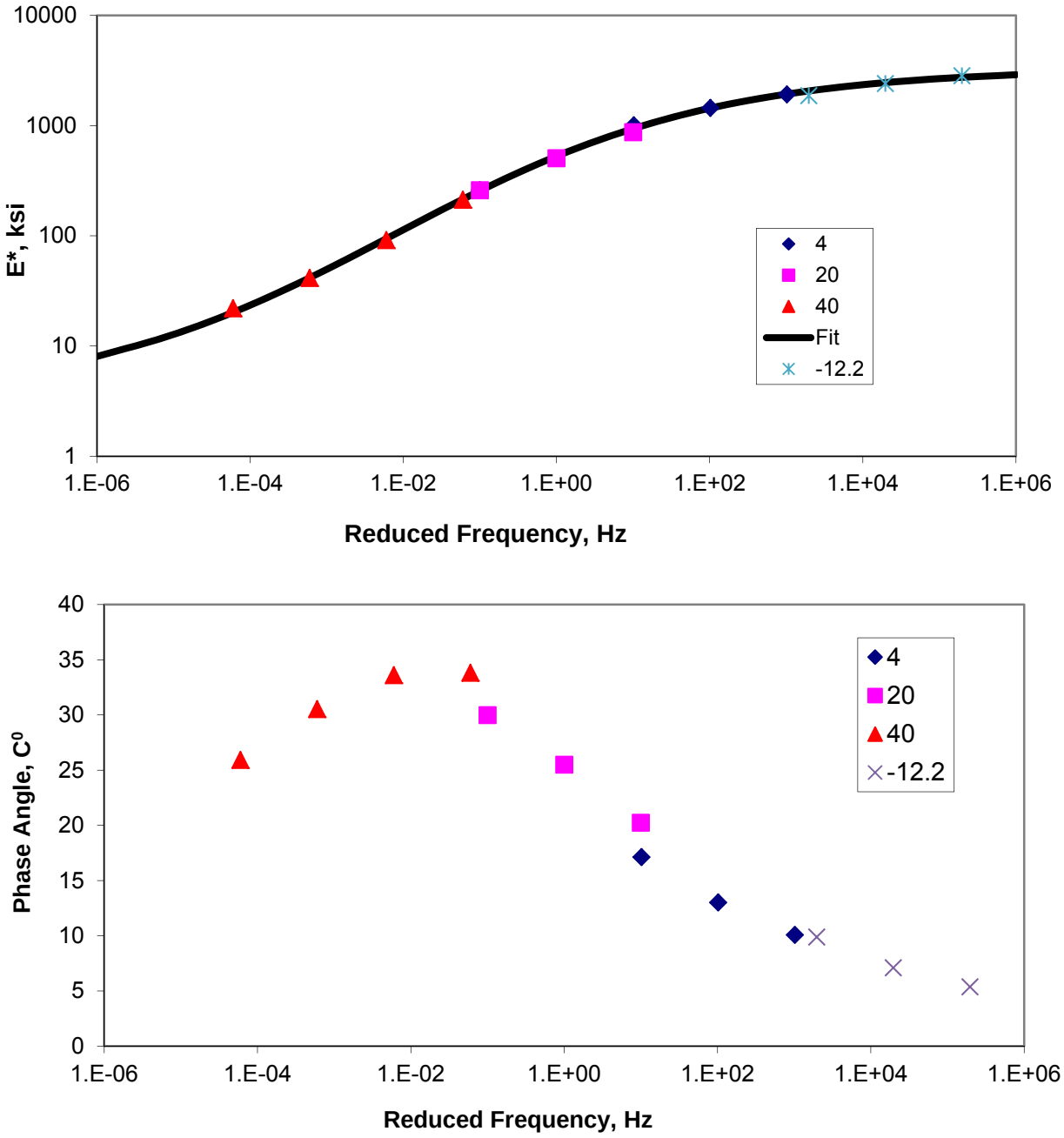

Figure 3. Master Curve for Mix A.

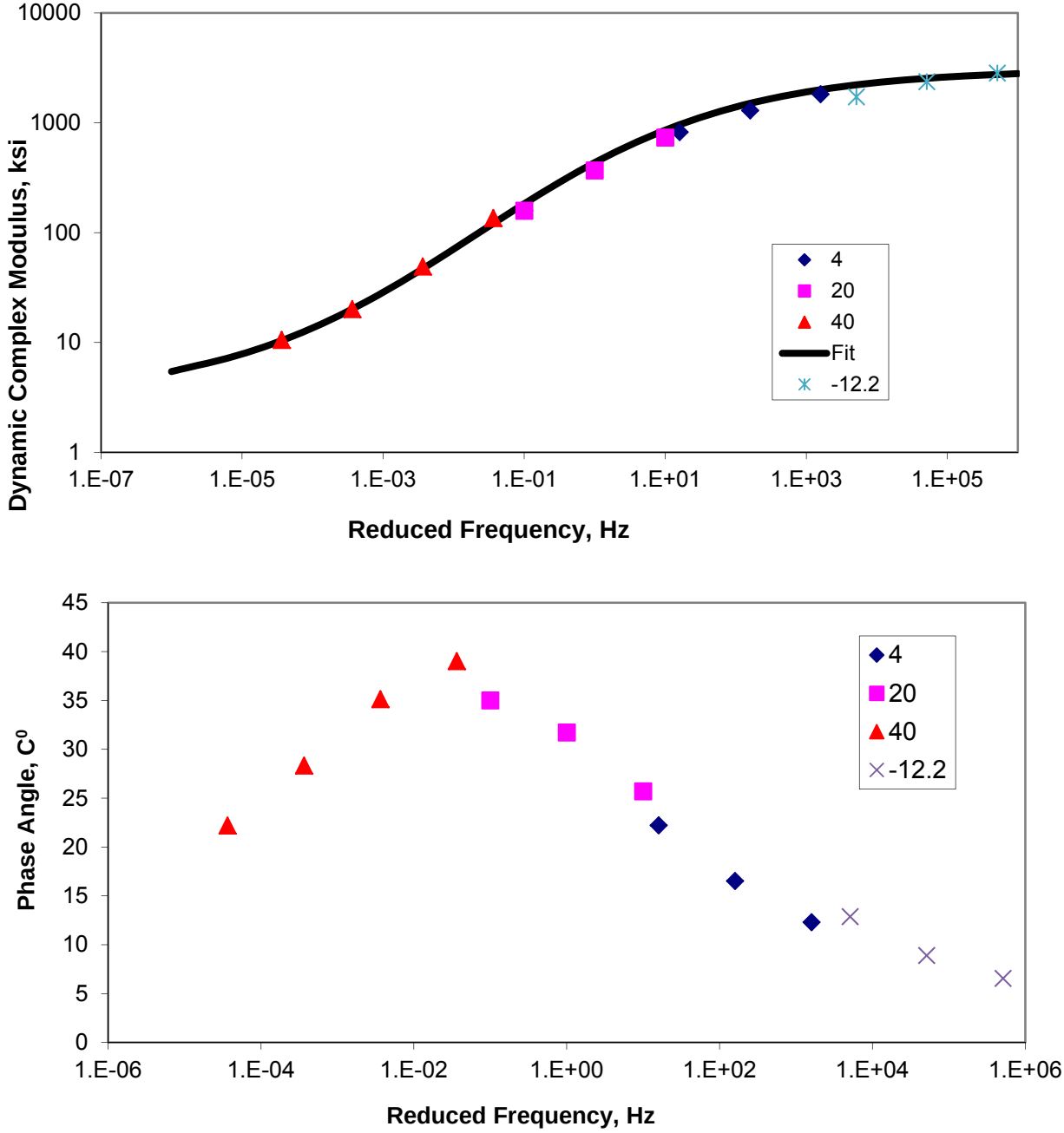

Figure 4. Master Curve for Mix B.

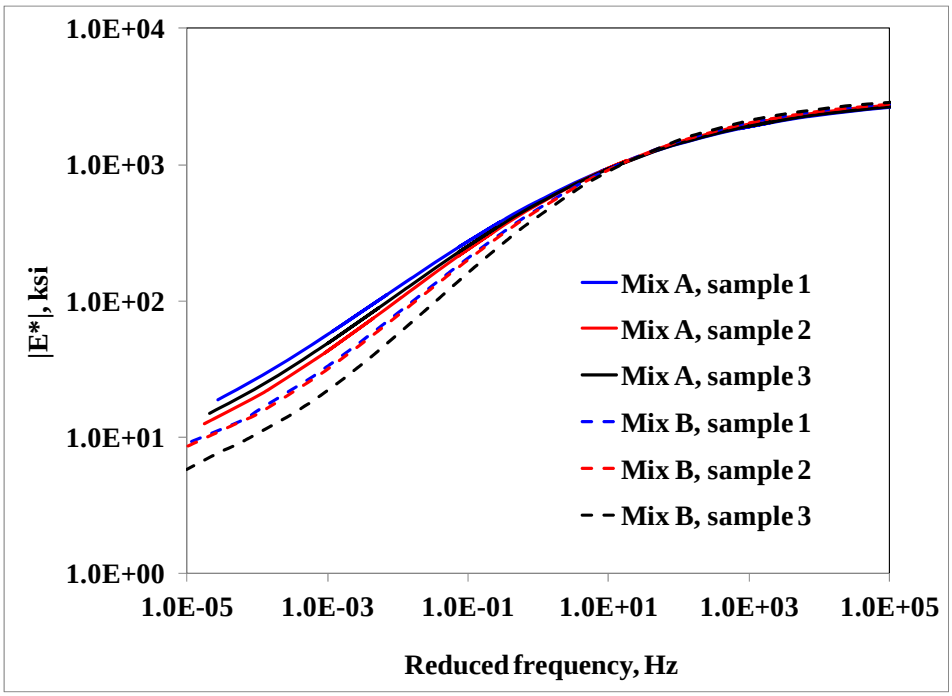

Figure 5. Dynamic Modulus Master Curves at a Reference Temperature of 77°F.

Disk-Shaped Compact Tension

The disk-shaped compaction tests were performed at 10°F, which was 10°C above the low PG grade of -22°C. A constant crack mouth opening displacement (CMOD) rate of 0.039 in./min was used. The specimens' fracture energy was determined by calculating the normalized area under the Load-CMOD curve. As shown in figure 3, the fracture energy of Mix B on average was 20% higher than mix A. The higher fracture energy might have resulted from the tighter gradation of mix B. The variability of the test results were within the allowable standard deviation values.

OVERLAY STRUCTURE, CONSTRUCTION, AND INSTRUMENTATION

Phase III test pavement consisted of control and interlayer sections. Prior to overlay construction, the milled concrete slab surface was thoroughly washed to remove all dirt and dust. To prevent interface slippage and secondary cracks, a thin tack coat of straight PG 64-22 asphalt was applied on the dry surface of two 12-in.-thick, 15- by 15-ft concrete slabs. On the basis of FEA simulation and laboratory test results, the interlayer section was designed as 1-in.-thick mix B HMA plus a 4-in.-thick overlay using standard FAA P-401 (PG 64-22) material. It was believed that this overlay thickness was sufficient above the softer interlayer to prevent rutting, slippage cracks, and shoving in the overlay areas where aircraft accelerate, decelerate, or make sharp turns. On the control section, the entire 5-in. overlay consisted of the same FAA P-401 material. Continuing from past successful experiments (59), each overlay was 30- by 5-ft with a 2-ft gap in between. To facilitate instrumentation, the overlay was built in multiple lifts (1.0, 1.5, and 2.5 in.). Between lifts, time was cautiously

balanced to allow for the application of a tack coat, placement of instrumentation sensors, and an adequate mix temperature to achieve the desired density. Thermocouples were embedded at various depths and locations to monitor the overlay temperature. There were unexplained spikes and dips in the temperature ranges that might have contributed to the tearing appearance in the interlayer surface. However, after compaction, the interlayer was smooth and stable.

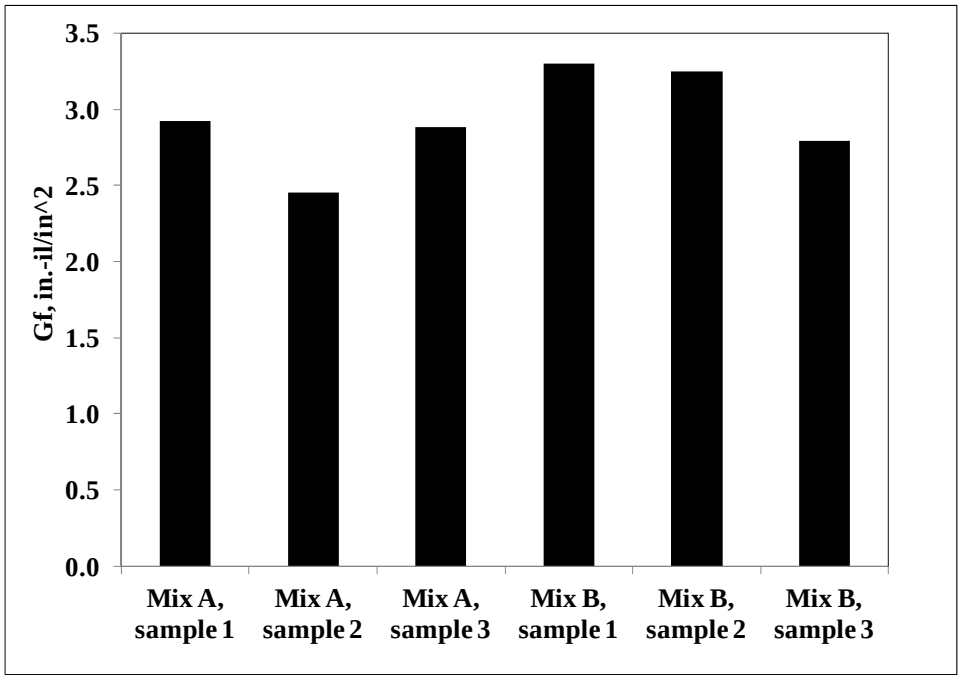

Figure 6. Fracture Test Results.

During the overlay paving, H-type asphalt strain gages (EG) were placed at the mid-depth (2.5 in.) of the overlay. Prior studies (61, 62) suggested potential interference between the embedded sensors and crack propagation. It was speculated that such a negative impact would be more prominent if the H-type sensors were installed in the 1-in.-thick interlayer. Alternatively, Fiber-Bragg Grating optical strain sensors were chosen because of their slim profile. One installation lesson learned was to cover the embedded sensors with material close to the lift thickness (i.e., 1-in.) and then use the screed of the paver to strike off the excess HMA to the proper depth and grade. As a result, instrumentation damage could be reduced to a minimum. After the overlay construction, surface strain gages (SG) were installed at various locations on the surface. A graphic sensor layout is shown in figure 7 and a complete array of installed strain sensors is given in table 6. Note that all sensors were installed on the “best guess” crack path, which was directly above and perpendicular to the concrete joint.

Table 6. Summary of Sensor Location and Cycle to Failure.

Overlay Section	Location in Overlay	Sensor ID	Cycle to Failure
Control	Bottom	FG6	2490
Control	Bottom	FG7	2026
Control	Bottom	SG14	4108
Control	Bottom	SG23	892
Control	Mid-depth	EG10	3004
Control	Mid-depth	EG12	2741
Control	Mid-depth	FG10	2477
Control	Mid-depth	EG14	2063
Control	Mid-depth	EG16	1967
Control	Mid-depth	SG15	4219
Control	Mid-depth	SG22	2955
Control	Surface	SG17	5173
Control	Surface	SG18	2815
Control	Surface	SG19	2254
Control	Surface	SG21	3196
Interlayer	Bottom	FG2	*
Interlayer	Bottom	FG3	*
Interlayer	Bottom	SG2	3257
Interlayer	Bottom	SG11	365
Interlayer	Mid-depth	EG2	2953
Interlayer	Mid-depth	EG4	2702
Interlayer	Mid-depth	FG9	2385
Interlayer	Mid-depth	EG6	1747
Interlayer	Mid-depth	EG8	1634
Interlayer	Mid-depth	SG3	3611
Interlayer	Mid-depth	SG10	2088
Interlayer	Surface	SG4	5047
Interlayer	Surface	SG6	2878
Interlayer	Surface	SG7	1882
Interlayer	Surface	SG9	3117**

* Malfunctioned after 1350 cycles
** From visual examination

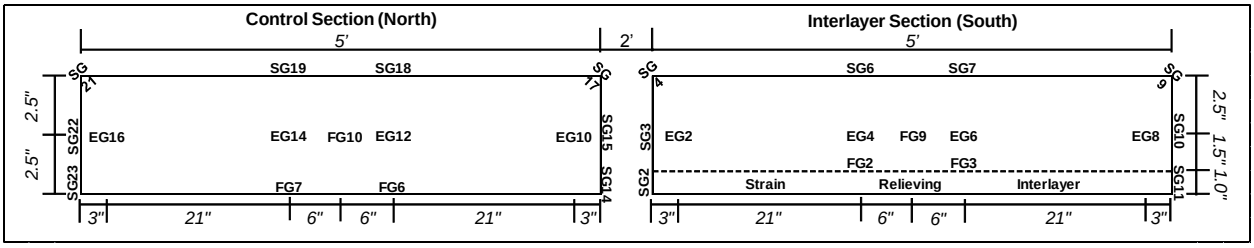

Figure 7. Strain Sensor Layout.

FULL-SCALE TEST

Full-scale tests began on June 3, 2014. The Phase III test employed the same test protocol as the Phase II test. The overlay bottom temperature was maintained at 32°F. The temperature variations were approximated by a haversine load waveform describing the relationship between the joint opening (0.012 in.) and cycle time (150 sec). At the end of each loading cycle, a rest (nonload) period of 600 sec was included to allow the overlay to relax. After 6350 cycles, the overlay was completely separated and the test concluded on July 30, 2014.

Performance of Fiber Optic Strain Sensor

As mentioned before, fiber optic strain sensor (FG) was introduced to the Phase III test. The FG provides active temperature compensation that is critical to temperature-dependent materials, such as AC. As illustrated in figure 8a, the most attractive feature of FG is its thin profile. In addition, a stainless steel carrier was used to secure and protect the fiber. Figure 8b shows the strain responses from both EGs and the FG during one loading cycle. In a side-by-side comparison with H-type EGs, the FG responses were equally sensitive and reasonable. However, the FG's slimness may result in unexpected failure. As shown in table 6, FGs 2 and 3 malfunctioned after only 1350 loading cycles.

Comparison of FEA and Field Responses

Figure 9 presents a comparison of horizontal tensile stresses obtained from FEA and field responses. Field stresses were calculated from active load cell readings and overlay cross sections. These load cell records came from the very beginning of the loading cycles; therefore, the responses from both sources represented an undamaged stress state in the overlay. As shown in figure 9, the FE model underpredicted horizontal tensile stresses at all locations. A better agreement between predicted and field responses was achieved, as upper points in the overlay were considered. The largest divergence between predictions and field values (about 27%) was observed at the overlay bottom on the interlayer section. One possible explanation is that perfect bonding was assumed between the interlayer, the overlay above it, and the concrete slabs below it. Laboratory characterization is needed to evaluate the mechanical characteristics of this bond, which in turn can be used to improve FEA predictions.

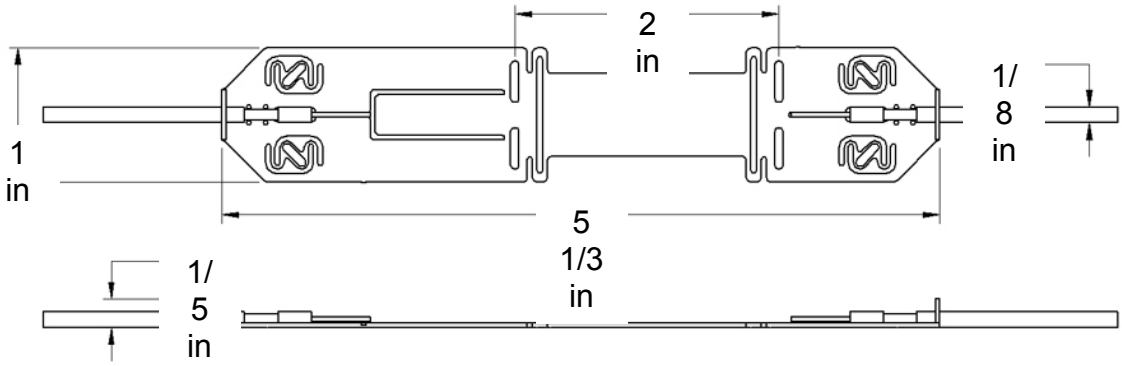

(a) Diagram

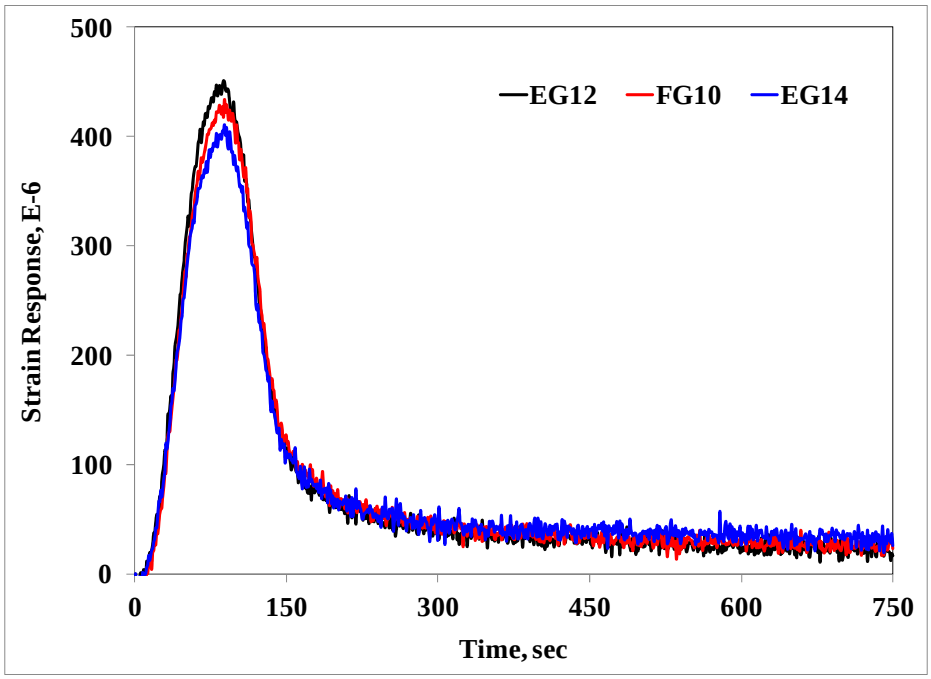

(b) FG vs. EG responses

(c)

Figure 8. Fiber Optic Strain Sensor.

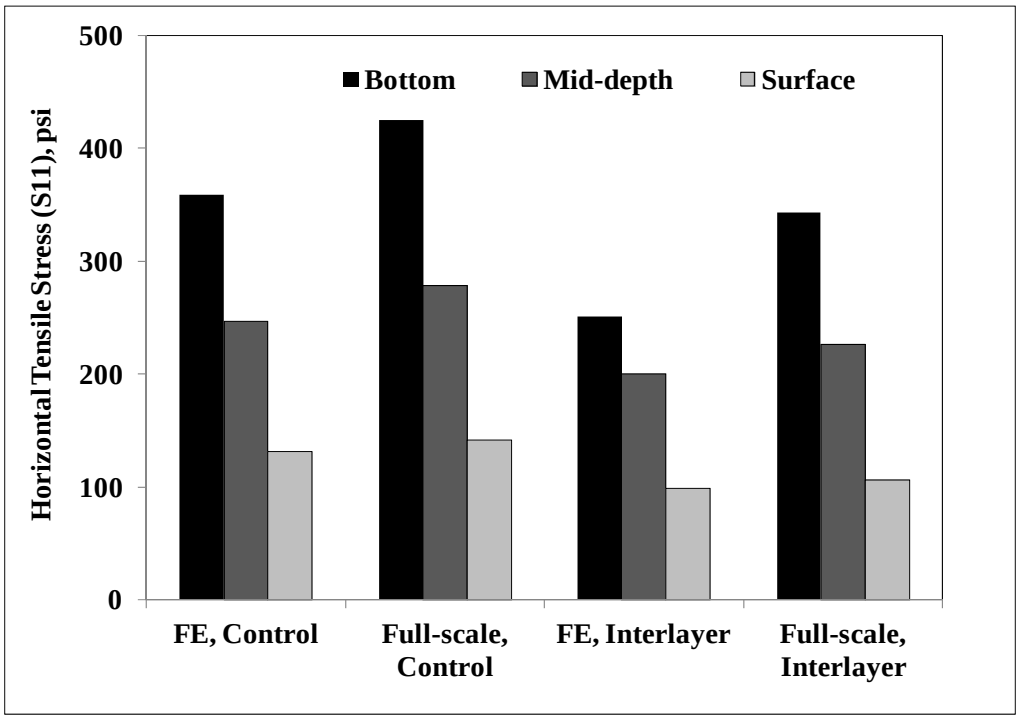

Figure 9. Comparison of FEA and Field Responses.

Crack Initiation

In view of previous successful experiments (2, 3), strain responses were used as the primary tool to determine crack initiation. In addition, a visual examination of the test pavement was conducted multiple times a day to identify cracks off the "best guess" crack path and trace the extension of existing cracks. For demonstration purposes, strain responses from one sensor at each depth were plotted, as shown in figure 10. All strain sensors except SG11 recorded that the tensile strain continuously grew at a slow rate and then experienced a rapid increase. A surface inspection revealed that SG11 was 0.5 in. away from the crack (figure 11a), but the other sensors were directly atop the crack (figure 11b). The abrupt drop in the strain response from SG11 was most likely caused by the strain energy released during crack formation. The intact interlayer shifted the maximum tensile stresses from the overlay bottom to the interlayer bottom. All failure strains recorded on the control section were consistent with the previous experiments (59-61).

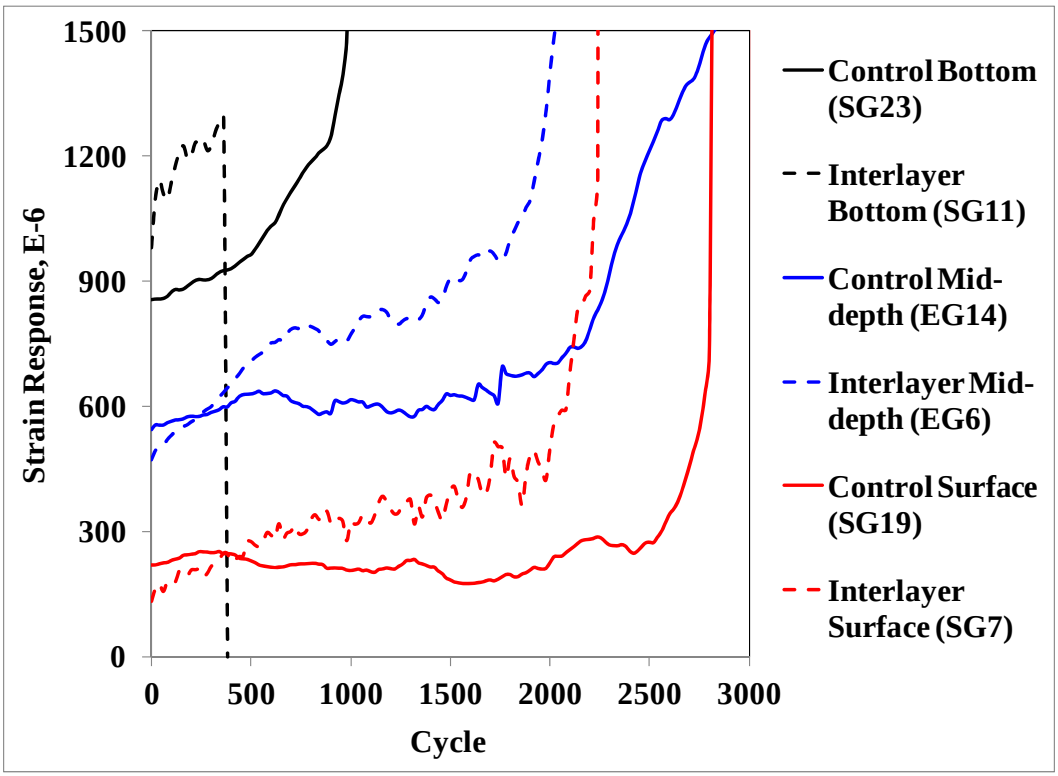

Figure 10. Strain Response History Plot.

Figure 11c depicts the third scenario in which the strain sensor was offset from the crack. Table 2 showed that SG9 was the only strain censor not able to detect the crack initiation. Monismith and Coetzee (32) and Button and Lytton (31) reported that, due to its low stiffness, the interlayer will exhibit large deformations, which are accompanied by a dissipation of energy that would otherwise be part of the crack propagation. This concept is demonstrated in figure 10, as the strain sensor at the overlay bottom registered much higher tensile strains on the interlayer section. When the bottom-up cracks propagated into the upper portion of the overlay, the soft interlay effect on the strain responses became less noticeable.

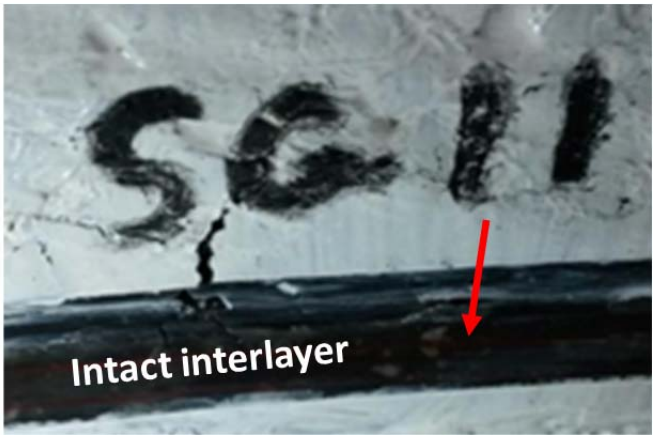

(a)

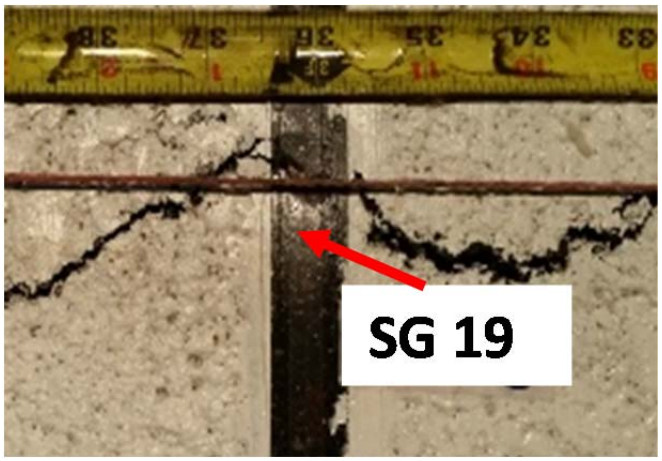

(b)

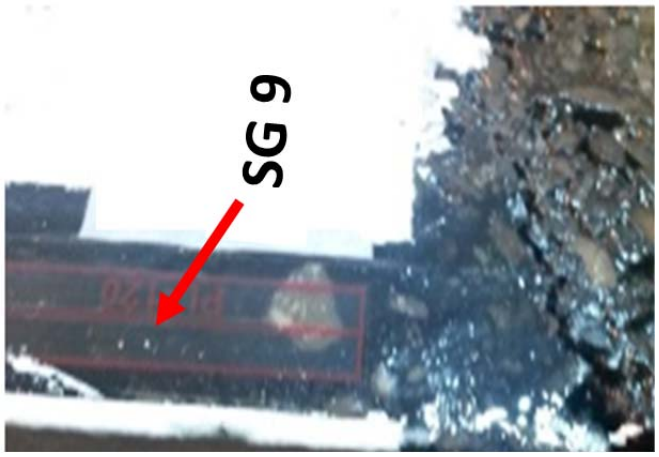

(c)

Figure 11. Crack Initiation.

Crack Propagation

The first through crack on the control section was captured by SG23, EG16, and SG19. On the interlayer section, strain responses from SG11, EG8, and SG7 indicated the earliest bottom-up crack arriving at the surface. In this study, the failure was defined as the first appearance of full-depth reflection crack on the overlay surface. Because the control and interlayer sections had a different overlay thickness (5-in. vs. 4-in.), the relationship between normalized crack length and number of cycles is shown in figure 12. For both control and interlayer sections, the crack length developed gradually at the beginning, and its propagation rate became higher and higher with the crack growth. At the middle of the overlay, the crack propagation stage underwent a transition from quiescent to aggressive. It is also evident in figure 12 that the interlayer section required constantly more load repetitions to penetrate the crack through the overlay. The strain relieving interlayer enhanced the reflective cracking resistance of the overlay. The effectiveness of strain relieving interlayer was more pronounced at an early stage of crack propagation and slowly diminished as the crack length increased. For the Phase III test pavement, the existence of a 1-in.-thick interlayer could maximally extend the overlay service life by 15%. It should be pointed out that the service life only referred to the number of temperature loading cycles that HMA overlay would withstand prior to the failure due to reflective cracking. Given that the interlayer did not completely fail after 3232 cycles, the intact interlayer had prevented spalling and moisture infiltration at the joint and therefore prolonged the structural integrity of the pavement.

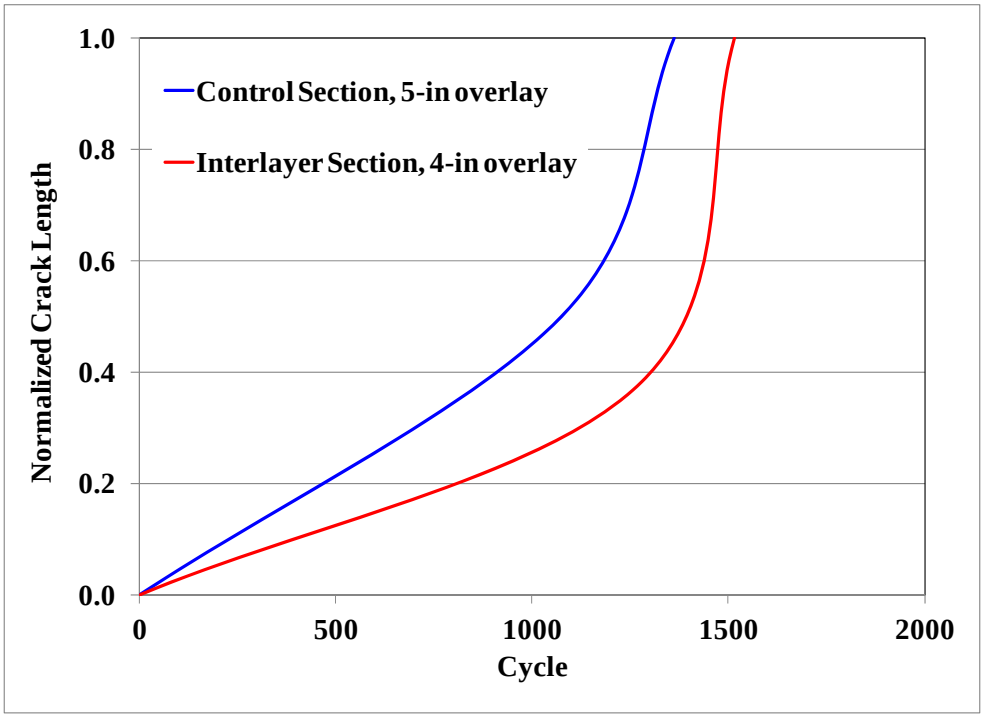

Figure 12. Crack Propagation.

Figures 13a and 13b show the overlay failure for the interlayer and control sections, respectively. On the interlayer section, the crack started above the intact interlayer. At first, the crack propagated upward, indicating fracture Mode I dominance. Once this vertical crack reached the 0.25-in. benchmark, it progressed in the horizontal direction, departing from the concrete joint until it reached the 1.0-in. benchmark. In the final stage,

the vertical crack progressed gradually on its initial path, and the horizontal crack started to deviate at an angle toward the surface. After 3117 cycles, the diagonal crack made an appearance on the overlay surface, 3.5 in. offset from the joint. At the same time, the vertical crack barely reached the 0.5-in. benchmark above the intact interlayer. It can be concluded that the fracture on the interlayer section was a mixed mode. On the control section, the reflection crack initiated from the overlay bottom and progressed on its upright track. The horizontal tensile stresses seemed to be the principal driving force for the overlay fracture in this case.

The above paragraph describes the bottom-up crack propagation in a vertical direction. It is worth noting that the reflection cracks had a tendency to develop across the overlay (along the joint) as well. When a Mode I crack formed and developed to a critical length, the energy release rate decreased. This decreasing driving force was due to the presence of compressive stresses in the inner portion of the overlay. As a result, in addition to the advance in the through-thickness direction, a bottom-up crack can advance in other orientations. This channeling phenomenon is reflected by the cycle to failure listed in table 2. Regardless of the depth, the crack occurrence was constantly observed earlier in the outer portion of the overlay than the inner portion.

(a) Interlayer section

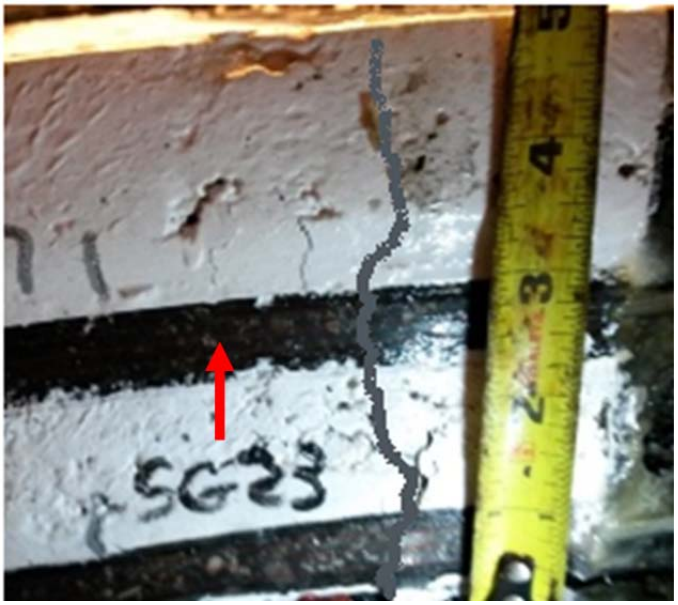

(b) Control section

Figure 13. Failure Observation.

CONCLUSIONS

Previous experiments at the FAA NAPTF identified that the critical zone to control bottom-up cracks was at the lower portion of the overlay. In Phase III Test the effectiveness of strain relieving interlayer to retard thermally-induced reflection cracks was evaluated. The interlayer HMA mix contained a highly polymerized asphalt binder (PG 76-22) and fine aggregate specially designed to absorb local straining generated directly above the concrete joint. The thickness and viscoelastic properties of the interlayer were determined from FEA and laboratory tests accordingly. Full-

scale tests were conducted on HMA overlays with and without an interlayer. Side-by-side comparisons of overlay performance led to the following conclusions:

1. The strain relieving interlayer enhanced the reflective cracking resistance of an HMA overlay. The effectiveness of strain relieving interlayer was more pronounced at an early stage of crack propagation and slowly diminished as the crack length increased.
2. Inclusion of a 1-in.-thick interlayer between existing concrete slabs and the overlay extended overlay service life up to 15%. The intact interlayer had prevented spalling and moisture infiltration at the joint and therefore prolonged the structural integrity of the pavement.
3. To realistically characterize the development of bottom-up reflection cracks, both mixed-mode fracture and crack channeling should be considered.

DATA STORAGE AND ORGANIZATION

Placeholder until RC Database in place

REFERENCES

1. Nunn, M.E. (1989) An Investigation into Reflection Cracking in Composite Pavements, *1st International RILEM Conference*.
2. Hughes, J.J. and Al-Qadi, I.L. (2001) Evaluation of Steel Paving Mesh, FHWA report.
3. Federal Aviation Administration (2009) AC 150/5320-6E, Airport Pavement Design and Evaluation.
4. USDOE, United States Department of Energy web page, Annual Energy Outlook (2000) Energy Information Administration, Available: http://www.eia.doe.gov/.
5. Huges, C. S. and McGhee, K. H. (1973) Results of reflective crack questionnaire survey, *Report No. VHRC 72-R25*, Virginia Highway Research Council.
6. Shalaby, A. and Fréchette, L. (2000) Reflective cracking on C-SHRP long term pavement performance sites, 4th RILEM International Conference on Reflective Cracking in Pavements.
7. Wei, C. and Tighe, S. (2004) Development of Preventive Maintenance Decision Trees Based on Cost-Effectiveness Analysis, *Journal of the Transportation Research Board, No. 1866*.
8. Barksdale, R. D. (1991) Fabrics in asphalt overlays and pavement maintenance, *NCHRP Report 171*, Transportation Research Board, Washington, D.C.
9. Lytton, R. L. (1989) Use of geotextiles for reinforcement and strain relief in asphalt concrete, *Geotextiles and Geomembranes, Vol. 8*.
10. Button, J. W. and Lytton, R. L. (2007) Guidelines for Using Geosynthetics with Hot-Mix Asphalt Overlays to Reduce Reflective Cracking, *Journal of the Transportation Research Board, No. 2004*.
11. Department of The Air Force (2001) Engineering Technical Letter (ETL) 01-9: Procedures to Retard Reflective Cracking.
12. Ellis, S. J. and Langdale, P.C. (2002) Performance of Techniques To Minimise Reflection Cracking and Associated Developments in Pavement Investigation for Maintenance of UK Military Airfields, *Federal Aviation Administration Airport Technology Transfer Conference*, Atlantic City, NJ.
13. Von Quintus, H.L., Mallela, J., Weiss, W., and Shen, S. (2009) Technical Guide AAPTP 05-04 Techniques for Mitigation of Reflective Cracks.
14. Deborah, A.C., Cheng, R., Eger, R.J., Grusczynski, L., Marlowe, J., Roohanirad, A., and Titi, H. (2004) Highway Preventive Maintenance Implementation: Comparing Challenges, Processes and Solutions in Three States, *Transportation Research Record No. 1877*.

15. Walter, P.K. and Bionda, R.A. (1990) Sawing and Sealing of Joints in Asphaltic Concrete Overlays, *Transportation Research Record No. 1268*.

16. Al-Qadi, I.L., Fini, E.H., Elseifi, M.A., Masson, J.F., and McGhee, K.M. (2006) Viscosity Determination of Hot-Poured Bituminous Sealants, *Transportation Research Board No. 1958.*

17. Brown, E.R., Mallick, R.B., Haddock, J.E., and Bukowski, J. (1997) Performance of Stone Matrix Asphalt Paving Mixtures (SMA) in the United States, *NCAT Report No. 97-01*, National Center for Asphalt Technology, Auburn, AL.

18. Al-Qadi, I. L., Elseifi, M., and Leonard, D. (2003) Development of an Overlay Design Model for Reflective Cracking with and without Steel Reinforcing Netting, *Journal of the Association of Asphalt Paving Technologists, Vol. 72.*

19. Al-Qadi, I. L. and Elseifi., M. A. (2004) Field Installation and Design Considerations of Steel Reinforcing Netting to Reduce Reflection of Cracks, *5th International RILEM Conference*.

20. Button, J. W. and Lytton, R. L. (2003) Guidelines for Using Geosynthetics with HMA Overlays to Reduce Reflective Cracking, *Report 1777-P2*, Texas Department of Transportation.

21. Ahlrich, R. C. (1986) Evaluation of Asphalt Rubber and Engineering Fabrics as Pavement Interlayers, *Final Report, Miscellaneous Paper GL-86-34*, U.S. Army Corps of Engineers, Waterways Experiment Station, Vicksburg, MS.

22. Buttlar, W., Dempsey, B., and Bozkurt, D. (1999) Evaluation of Reflective Crack Control Policy, *Report No. ITRC FR 95/96-4*, Illinois Department of Transportation.

23. Maurer, D. and Malasheskie, G. (1989) Field Performance of Fabrics and Fibers to Retard Reflective Cracking, *Transportation Research Record No. 1248*.

24. Amini, F. (2005) Potential Applications of Paving Fabrics to Reduce Reflective Cracking, *Final Report FHWA/MS-DOT-RD-05-174*, Department of Civil & Environmental Engineering, Jackson State University.

25. Epps, J.A. and Button, J.W. (1984) Fabrics in Asphalt Overlays-Design, Construction and Specifications, *Report No. 261-3F*, Texas Transportation Institute.

26. Button, J. (1989) Overlay Construction and Performance Using Geotextiles, *Transportation Research Record No. 1248*.

27. Bozkurt, D., Buttlar, W., and Dempsey, B. (2000) Cost-Effectiveness of Reflective Crack Control Treatments in Illinois, *4th International RILEM Conference*.

28. Shuler, S., and Harmelink, D. (2004) Reducing Reflection Cracking in Asphalt Pavements, *5th International RILEM Conference*.

29. Soucie, T. (2007) Experimental Installation of Geosynthetic Pavement Reinforcement to Reduce Reflective Cracking, *Report No. 01-3*, Transportation Research Division, Maine Department of Transportation.

30. Ramsamooj, D. V. and Gabriel, J. (1998) Airport Rehabilitation Using Asphalt Concrete/Fiberglass Composite Overlays, *Second International Conference on Composites in Infrastructure*.

31. Button, J. W. and Lytton, R. L. (1987) Evaluation of fabrics, fibers and grids in overlays, *6th International Conference on Structural Design of Asphalt Pavements, Vol. 1*.

32. Monismith, C. L. and Coetzee, N. F. (1980) Reflection cracking: analysis, laboratory studies and design considerations, *Journal of the Association of Asphalt Paving Technologists, Vol. 49*.

33. Zhengqi, Z. and Denglaing, Z. (2000) Evaluation of Geonet Reinforcement in Resisting Reflective Cracking of Asphalt Pavement, *4th International RILEM Conference*.

34. Brown, S. F., Thom, N. H., and Sanders, P. J. (2001) A Study of Grid Reinforced Asphalt to Combat Reflection Cracking, *Journal of the Association of Asphalt Paving Technologists, Vol. 70*.

35. Montestruque, G., Rodrigues, R., Nods, M., and Elsing, A. (2004) Stop of Reflective Crack Propagation with the Use of Pet Geogrid as Asphalt Overlay Reinforcement, 5th *International RILEM Conference*.

36. Gallego, J. and Prieto, J. N. (2006) New Laboratory Equipment for Study of Reflective Cracking in As-phalt Overlays, *85th Annual Meeting of the Transportation Research Board*, Washington, D.C.

37. Dave, E. V., Song, S. H., Buttlar, W. G., and Paulino, G. H. (2007) Reflective and Thermal Cracking Modeling of Asphalt Concrete Overlays, *International Conference of Advanced Characterisation of Pavement and Soil Engineering Materials, Vol. 1*.

38. Kim, M., Buttlar, W.G., Baek, J., and Al-Qadi, I. L. (2009) Field and Laboratory Evaluation of Fracture Resistance of Illinois HMA Overlay Mixtures, *Transportation Research Record No. 2127*.

39. Buttlar, W.G., Dave, E.V., and Sherman, D.S. (2010) Hybrid Reflective-Crack Relief System at Greater Peoria Regional Airport: A Case Study, *FAA Technology Transfer Conference*.

40. Dave, E.V., Ahmed, S., Buttlar, W.G., Bausano, J.P., Lynn, T. (2010) Investigation of Strain Tolerant Mixture Reflective Crack Relief Systems: an Integrated Approach, *Journal of the Association of Asphalt Paving Technologists, Vol 79.*

41. Majidzadeh, K. (1976) A laboratory investigation of the use of Petromat for optimization of pavement performance, Ohio State University, Sponsored by Phillips Petroleum Company.

42. McLaughlin, A.L. (1979) Reflection Cracking of Bituminous Overlays for Airport Pavements, A State of the Art, *Report No. FAA-RD-79-57*. Federal Aviation Administration.

43. Way, G. B. (1980) Prevention of Reflective Cracking in Arizona, *Journal of the Association of Asphalt Paving Technologists, Vol. 49*.

44. Vedros, P. J. (1981) Evaluation of Membrane Interlayers for Prevention of Crack Reflection in Thin Overlays, *Miscellaneous Paper GL-81-8, U.S. Army Corps of Engineers Waterways Experiment Station, Vicksburg, MS.*

45. Sherman, G. (1982) Minimizing Reflection Cracking of Pavement Overlays, *Transportation Research Board, NCHRP Synthesis of Highway Practice 92*.

46. Paterson, W. (1983) Design Study of Asphalt Membrane-Overlay for Concrete Runway Pavement, *Transportation Research Record No. 930.*

47. McKeen, R. G., Newcomb, D. E., and Hanson, D. I. (1984) Material Characterization and Design Considerations for Membrane Interlayers, *Journal of the Association of Asphalt Paving Technologists, Vol. 53*.

48. Barksdale, R.D.; Brown, S.F.; and Chan, F. (1989) Potential Benefits of Geosynthetics in Flexible Pavements, *NCHRP Report 315*, Transportation Research Board, Washington, D.C.

49. Mukhtar, M. T. (1994) Interlayer Stress Absorbing Composite (ISAC) for Mitigating Reflection Cracking in Asphalt Concrete Overlays, Ph.D. Dissertation, University of Illinois at Urbana-Champaign, Urbana, IL.

50. Dempsey, B. J., and Mukhtar, M. T. (1997) Interlayer Stress Absorbing Composite in AC Overlays, *Aircraft/Pavement Technology In the Midst of Change, pp. 244-258*.

51. Dempsey, B. J. (2002) Development and Performance of Interlayer Stress-Absorbing Composite in Asphalt Concrete Overlays, *Transportation Research Record No. 1809.*

52. Vespa, J. W. (2005). An Evaluation of Interlayer Stress Absorbing Composite (ISAC) Reflective Crack Relief System, *Final Report, FHWA/IL/PRR 150*, Illinois Department of Transportation.

53. Al-Qadi, I.L., Buttlar, W.G., Baek, J., and Kim, M. (2009) Cost-effectiveness and Performance of Overlay Systems in Illinois, Volume I: Effectiveness Assessment of HMA Overlay Interlyer Systems Used To Retard Reflective Cracking, *Research Report ICT-09-044*, Illinois Center for Transportation.

54. Al-Qadi, I.L., Buttlar, W.G., Baek, J. (2009) Cost-effectiveness and Performance of Overlay Systems in Illinois, Volume II: Guidelines for Interlayer System Selection Decision When Used in HMA Overlays, *Research Report ICT-09-045*, Illinois Center for Transportation.

55. Blankenship, P., Drbohlav, J., and Iker, N. (2003) Interlayer and Design Considerations to Retard Reflective Cracking, *Proceedings of the 81st Annual Meeting of the Transportation Research Board*.

56. Elseifi, M. and Al-Qadi, I. L. (2005) Effectiveness of Steel Reinforcing Netting in Combating Fatigue Cracking in New Flexible Pavement Systems, *Journal of Transportation Engineering, ASCE, Vol. 131, No. 1*.

57. Yin, H. and Barbagallo, D. (2013) Development of Full-Scale Reflective Cracking Test at FAA NAPTF, *Transportation Research Record No.2368*, Washington, DC.

58. Yin, H. (2013) Finite Element Modeling and Analysis of Full-Scale Reflective Cracking Test, *International Journal of Roads and Airports*.

59. Yin, H. (2014) Full-Scale Test of Thermally-Induced Reflective Cracking in Airport Pavements, *International Journal of Road Materials and Pavements Design, Vol 16*.

60. Federal Aviation Administration (2017) Reflective Cracking Phase I Test Report.

61. Federal Aviation Administration (2017) Reflective Cracking Phase II Test Report.

62. Yin, H. (2013) The Impact of Strain Gage Instrumentation on Localized Strain Responses in Asphalt Concrete Pavements, *International Journal of Pavement Research and Technology*.

APPENDIX A—HMA Mix Specification for Strain Relieving Interlayer

The main purpose of a strain relieving interlayer is to isolate relative displacements between the overlay and existing pavement such that the longitudinal horizontal tensile stresses in the overlay caused by thermal cycling can be significantly reduced. Furthermore, the interlayer shifts the maximum tensile and shear stress from the bottom of the overlay to the bottom of the interlayer, as long as the interlayer is intact. To accomplish these functions, the interlayer material must possess excellent strain relieving properties and have the ability to relax stresses rapidly. The strain relieving interlayer should be a fine graded, polymer modified binder (PMA), asphalt-rich mixture. The PMA is a cross-linked elastomeric styrene-butadiene block copolymer system and the aggregate consists of crushed fines and screenings. The PMA is less temperature susceptible and has higher viscosity at ambient temperature when compared to unmodified or neat asphalt mixtures. In addition, the PMA gives the elasticity to withstand and partially absorb the tension, shear and bending exerted on the pavement.

DESCRIPTION

This specification covers materials and construction requirements for producing and placing **two** HMA mixtures to be placed in one lift atop concrete pavements. The mixture shall be a highly elastic, impermeable HMA that is designed to reduce thermally-induced reflective cracking. The interlayer shall be applied with paving and compaction equipment (paving and roller) directly on the existing PCC. The interlayer shall be covered with a conventional HMA overlay in conformance with the lines, grades, and typical cross sections shown on the plans.

MATERIALS

All materials shall conform to the requirements listed herein, unless otherwise noted.

Bituminous Material

The asphalt binder shall meet the requirements of AASHTO M320 with a PG high temperature of 76°C and low temperature of -22°C. In addition, the asphalt binder shall meet the following:

Test	**Criteria**
RTFO Elastic Recovery (ASTM D6084)	75% minimum @ 25°C
Separation (ASTM D5976)	6°C difference max. after 48 hr.

Aggregate

Aggregates shall consist of crushed stone, crushed gravel, or crushed slag without natural sand or other inert finely divided mineral aggregate. Recycled Asphalt Pavement (RAP), or other reclaimed materials, shall not be used. The portion of combined materials retained on the No. 4 sieve is coarse aggregate and shall meet the following requirements:

- Wear (tested in accordance with ASTM C 131) shall not be greater than 40%;
- Sodium Sulfate Soundness (tested in accordance with ASTM C 88) shall not exceed 10%; and
- Flat, elongated and flat & elongated particles (tested in accordance with ASTM D 4791 at 5:1) shall not exceed 8%.

The portion of the combined materials passing the No. 4 sieve and retained on the No. 200 sieve is fine aggregate and shall meet the following requirements:

- Plasticity Index less than 6 and Liquid Limit less than 25 (tested in accordance with ASTM D 4318);
- Sand Equivalent (tested in accordance with AST D 2419) greater than 45; and
- Fine Aggregate Angularity (tested in accordance with ASTM C 1252) greater than 45.

Additionally, the blended aggregates shall meet the gradation ranges shown below. The contractor shall provide the types and sources of all aggregate components, gradations of the individual aggregate components, the relative percentage of each component in the proposed blend, and the optimum asphalt content (AC) Superpave design required to meet all specification requirements. The maximum deviation from the approved job mix formula (JMF) based on an average of five samples shall be as follows:

Sieve Size	**Percent Passing**		
	Mix A	**Mix B**	**Tolerance**
⅜ in. (9.5 mm)	100	100	-
No. 4 (4.75 mm)	75 – 100	90 – 100	-
No. 8 (2.36 mm)	30 – 85	55 – 90	± 4.0
No. 16 (1.18 mm)	-	-	-
No. 30 (0.600 mm)	-	20 – 55	-
No. 50 (0.300 mm)	-	-	-
No. 100 (0.150 mm)	-	-	-
No. 200 (0.075 mm)	6 – 14	4 – 10	± 1.4

Composition

The plant HMA shall be composed of a mixture of aggregate, filler and anti-strip agent if required, and bituminous material. The several aggregate fractions shall be sized, handled in separate size groups, and combined in such proportions that the resulting mixture meets the grading requirements of the JMF.

Mixture Testing

The interlayer mixture shall be designed in accordance with AASHTO R35, *Standard Practice for Superpave Volumetric Design for Hot Mix Asphalt*, and tested in accordance with AASHTO T-312, *Preparing and Determining the Density of Hot Mix Asphalt specimens by means of the Superpave Gyratory Compactor,* except as noted herein. Fifty gyrations (N_{design}= 50) shall be required for gyratory compaction (NO N_{ini} or N_{max} testing are required).

JMF Acceptance Criteria

The JMF shall meet the following volumetric and performance requirements:

HMA Mix	**Density (% of Max Sp. Gr.)**	**Criteria**							
		Asphalt Content (AC), %		**Air Void (Va), %**		**Voids in Mineral Aggregate (VMA), %**		**Mixing Temperature**	**Compaction Temperature**
		Target	Tolerance	Target	Tolerance	Target	Tolerance		
A	93-94	≥ 7	± 0.3	1 - 3	± 0.8	≥ 16	-1	< 360 °F	> 275 °F
B				3-4	± 0.5	≥ 18			

Laboratory mixing and compaction temperatures should be used during the HMA mixture design shall conform the above requirements.

CONSTRUCTION

Thickness

The interlayer shall be placed at a thickness of 1 inch with a tolerance of (±) 1/4 inch.

Temperatures

The Interlayer mixture shall never be mixed hotter than 180°C (360°F). The interlayer mixture must be compacted at temperatures greater than 135°C (275°F). The production and placement temperatures should be carefully controlled so that adequate densities can be obtained. Without adequate compaction,

insufficient fracture properties will be obtained eliminating the benefit of using PMA.

Test Batch and Strip

At least one full day prior to full production, the contractor shall prepare a quantity of bituminous mixture according to the approved job mix formula. The amount of mixture should be sufficient to construct **two** test sections (Mix A and B) at least 50 ft long and 5 ft wide. The equipment to be used in construction of the test sections shall be the same type and weight to be used on the job site at the FAA NAPTF.

Compaction and Density

Compaction operations shall start promptly after placement of the interlayer mixture. **Only** steel wheel rollers in the static mode shall be used for compaction of the mixture. Density of the in-place interlayer shall be **between 93.0% and 94.0%** of the maximum specific gravity (G_{mm}) as determined by AASHTO T-209, *Theoretical Maximum Specific Gravity and Density of Bituminous Paving Mixtures.* Density shall be determined by a thin-lift nuclear density gage.

Weather Limitations

The interlayer shall not be placed when the temperature of the surface on which the interlayer will be placed is less than 10°C (50°F). The interlayer shall not be placed on a wet or damp surface.

Application of Tack Coat

A hot asphalt cement tack coat shall be applied uniformly at the rates shown below and at a spraying temperature of 163°C. The tack coat shall conform to grade PG 64-22 asphalt binder. The contractor shall be capable of applying straight asphalt binder uniformly across the pavement surface at the rates and temperatures specified. The spraying temperature and application rate will be adjusted as required to produce a uniform coating so that every part of the surface is covered, with no excess material. A tack coat shall also be placed atop the interlayer at the smooth surface application rates shown below prior to placement of the HMA overlay.

Tack Coat	**Smooth Surfaces, gal/sy**	**Milled Surfaces, gal/sy**
PG 64-22	0.04 to 0.06	0.06 to 0.08

REPORT

The job mix formula shall be submitted in writing by the Contractor to the Engineer at least 30 days prior to the start of paving operations and shall include as a minimum:

a) Percent passing each sieve size for total combined gradation, individual gradation of all aggregate stockpiles and percent by weight of each stockpile used in the job mix formula.
b) Percent of asphalt cement.
c) Asphalt performance, viscosity or penetration grade, and type of modifier if used.
d) Compaction temperature.
e) Temperature of mix when discharged from the mixer.
f) Temperature-viscosity relationship of the asphalt cement.
g) Plot of the combined gradation on the Federal Highway Administration (FHWA) 45 power gradation curve.
h) Percent fractured faces.
i) Percent by weight of flat particles, elongated particles, and flat and elongated particles (and criteria).
j) Tensile Strength Ratio (TSR).
k) Anti-strip agent (if required).
l) Date the job mix formula was developed.

The Contractor shall submit to the Engineer the results of verification testing of three (3) asphalt samples

prepared at the optimum asphalt content. The average of the results of this testing shall indicate conformance with the job mix formula requirements. When the project requires asphalt mixtures of differing aggregate gradations, a separate job mix formula and the results of job mix formula verification testing must be submitted for each mix.

U.S. Department of Transportation
ITS Joint Program Office-HOIT
1200 New Jersey Avenue, SE
Washington, DC 20590

Toll-Free “Help Line” 866-367-7487
www.its.dot.gov

[FHWA Document Number]

U.S. Department of Transportation